

R. & M. No. 3576



MINISTRY OF TECHNOLOGY

AERONAUTICAL RESEARCH COUNCIL
REPORTS AND MEMORANDA

A Momentum Analysis of Lifting Surfaces in Inviscid Supersonic Flow

By P. L. ROE

LIBRARY
ROYAL AIR FORCE ESTABLISHMENT
RECORD

LONDON: HER MAJESTY'S STATIONERY OFFICE

1969

PRICE 17s. 6d. NET

A Momentum Analysis of Lifting Surfaces in Inviscid Supersonic Flow

By P. L. ROE

*Reports and Memoranda No. 3576**
May, 1967

Summary.

Momentum considerations are used to derive relationships between the lifting efficiency of a wing having an attached shock system and properties of the flow field around it. Optimum two-dimensional flow fields are derived using shock expansion theory. These may be used to design three-dimensional shapes having slightly greater lifting efficiencies than plane wedges. An analysis of the flow in any plane of symmetry is used to suggest desirable features of more general flow fields.

LIST OF CONTENTS

Section.

1. Introduction
2. Momentum Relationships
3. A Property of the Lift and Drag Functions
4. Two-Dimensional Flow Fields
 - 4.1. Flows past plane wedges
 - 4.2. Optimum two-dimensional flow fields
5. Flow in a Plane of Symmetry
 - 5.1. Statement of the problem
 - 5.2. Optimum streamlines behind a given shockwave
 - 5.3. Optimum shock strength
 - 5.4. Discussion
6. Some Miscellaneous Applications
 - 6.1. Wings with unswept trailing edges supporting flow fields with axial symmetry
 - 6.1.1. Basic equations
 - 6.1.2. Variations of lift and drag functions away from central plane
 - 6.1.3. Relationship between lift and flow deflection
 - 6.1.4. References to other work

*Replaces R.A.E. Technical Report 67 124—A.R.C. 29530.

- 6.2. 'Mapping' of flow fields
- 6.3. On different types of flow field
- 6.4. Effects of trailing edge sweep
- 6.5. A possible experimental application
7. Future Work
8. Conclusions

List of Symbols

References

Appendix A Some simple oblique shock relationships

Appendix B The orders of magnitude of the terms in the drag function

Appendix C The effect of trailing edge sweep on a 'double-Nonweiler' wing

Illustrations—Figs. 1 to 25

Detachable Abstract Cards

1. *Introduction.*

A high lift-drag ratio is an important requirement for the efficient operation of any cruising aircraft. In the supersonic speed range, it is probably most important at low Mach numbers, where the well-developed methods of linear theory are fortunately available to indicate suitable lifting shapes. At high cruising speeds, it seems that purely aerodynamic design will be increasingly compromised by propulsion considerations, and by structural difficulties associated with kinetic heating. If it is assumed that some speed range exists, above that where linear theory provides an adequate description of the flow, and yet where worthwhile benefits are still to be gained from aerodynamic sophistication, it seems that new techniques must be adopted to investigate this region.

At the present time it seems probable that such a region does exist between Mach numbers limited roughly by 3 and 10. A general design philosophy appropriate to this speed range has been presented by Küchemann¹, of whose conclusions the most relevant to the present work is this; that an aircraft sufficiently highly swept to be aerodynamically slender at cruise will be unmanageable at low speeds, so that if we wish to avoid the complications associated with variable geometry, we must accept shapes whose leading-edge shock waves are either attached or nearly so (Fig. 1).

A promising technique²⁻⁶ for the theoretical investigation of such shapes involves 'freezing' stream surfaces in two-dimensional or axisymmetric flows, and patching them together to form lifting bodies whose near-field flow properties can be calculated exactly for design speed and attitude in an inviscid fluid. This method takes advantage of the fact that in supersonic aerodynamics inverse problems are often easier to solve than direct ones. Here one calculates not the flow past a given shape, but a shape which will support a given flow.

It would seem that questions concerning the lifting efficiencies of these shapes might also be best posed in an inverse fashion. That is to say we do not directly seek efficient shapes, but enquire rather in what manner an efficient shape should act on the air passing close to it. The present Report explores this idea by relating the lift and drag of a wing to the changes of pressure and momentum along nearby streamlines. Although the general optimisation problem is intractable, a number of interesting and suggestive results can be obtained. In particular, optimum flow processes can be calculated for individual streamlines which lie in a plane of symmetry, and optimum wing shapes can be derived in two-dimensional flows if shock-expansion theory is assumed valid.

All the analysis is performed on an assumption of zero base drag and no skin friction. No attempt is made to assess any aerodynamic properties other than the coefficients of lift and pressure drag based on planform area. Attention has been concentrated on the design of compression surfaces, since these are likely to be of prime importance in the speed range of interest.

2. Momentum Relationships.

We enclose the wing surface to be studied within a control box through which the momentum flux may be calculated. Each streamline passing through the box will be shown to be associated with certain functions which represent the contributions of the local flow to the overall forces.

The control volume is shown in Fig. 2, for an aircraft in straight and level flight. Two boxes are drawn, one to each surface of the wing, and each is formed of three surfaces. These are the surface of the wing, the forward envelope of the disturbances from that surface (either a shock or a Mach wave), and a surface composed of vertical generators drawn through the trailing edge.

For simplicity we consider only the lower box (V_1), the analysis for V_2 being evidently identical. This part of the box is redrawn and labelled in Fig. 3. It is convenient to define the frontal projection of $LTST'$ as the *capture area*, the frontal projection of $BTST'$ as the *exit area*, and the vertical projection of $LTBT'$ as the *planform area*. Also let the frontal projection of $LTBT'$ be the *base area* (A_b).

Consider the streamtube which enters the control volume through a small closed curve drawn on the shockwave (see Fig. 3). This small curve, when seen from in front, encloses an element dA_c of capture area, and when seen from above, an element dA_p of planform area. The same streamtube will leave the control volume through another small closed curve, which will lie this time in the surface TBT' , and this curve, when viewed from in front, encloses an element dA_e of exit area. It is also convenient to make use of another elemental area. This is the cross-section area of the streamtube, at the point where it leaves the control volume, measured normal to the free stream. This area, which, as shown in Fig. 3, is not in general equal to dA_e , will be called dA_e^* .

The net pressure forces on the lower surface are

$$L = \int_{LTBT'} (p_s - p_\infty) dA_p \quad (1)$$

$$D = \int_{LTBT'} (p_s - p_\infty) dA_b \quad (2)$$

where p_s is the static pressure on the surface.

Alternative expressions are easily written by use of the momentum theorem.

$$L = \int_{BTST'} \rho v_x v_z dA_e^* \quad (3)$$

$$D = \int_{LTST'} \rho_\infty v_\infty^2 dA_c - \int_{BTST'} \rho v_x^2 dA_e^* - \int_{BTST'} (p - p_\infty) dA_e \quad (4)$$

In these equations, a co-ordinate system (x,y,z) as shown in Fig. 3 has been employed, and the quantities v_x, v_z, p and ρ are all measured in the surface TBT' .

Now write $\frac{1}{2} \rho_\infty v_\infty^2$ as q_∞ and put equations (3) and (4) into coefficient form thus:

$$C_L = \frac{L}{q_\infty A_p} = \frac{1}{A_p} \int_{BTST'} \frac{\rho v_x v_z}{q_\infty} dA_e^* \quad (5)$$

$$C_D = \frac{D}{q_\infty A_p} = 2 \frac{A_c}{A_p} - \frac{1}{A_p} \int_{BTST'} \left\{ \frac{\rho v_x^2}{q_\infty} \left(\frac{dA_e^*}{dA_p} \right) + \frac{(p-p_\infty)}{q_\infty} \right\} dA_e. \quad (6)$$

The integrals here are evaluated over the exit area, but by making use of the one-to-one correspondence indicated above between elements of planform and exit area, we may transform equations (5) and (6) so that the integration is carried out over the planform area, then

$$C_L = \frac{1}{A_p} \int_{A_p} \frac{\rho v_x v_z}{q_\infty} \left(\frac{dA_e^*}{dA_p} \right) dA_p \quad (7)$$

which may be written:

$$C_L = \frac{1}{A_p} \int_{A_p} f_L dA_p \quad (8)$$

where

$$f_L = \frac{\rho v_x v_z}{q_\infty} \frac{dA_e^*}{dA_p}. \quad (9)$$

Equation (9) defines, for each streamline passing through the control volume, a 'lift function', and equation (8) shows that the lift coefficient of any wing is the mean value of the lift functions for the streamlines which it captures. In a similar manner, we define a 'drag function', f_D , such that

$$C_D = \frac{1}{A_p} \int_{A_p} f_D dA_p \quad (10)$$

where

$$f_D = 2 \frac{dA_c}{dA_p} - \frac{\rho v_x^2}{q_\infty} \frac{dA_e^*}{dA_p} - \frac{(p-p_\infty)}{q_\infty} \frac{dA_e}{dA_p}. \quad (11)$$

Equations (8) to (11) are the fundamental results on which the work in this Report is based. Through them, it is possible to consider the aerodynamic forces on a wing in relation to the flow field around it, rather than the surface pressures on it.

The remainder of this Section is devoted to simplifying the right hand sides of equations (9) and (11). To do this we need the relationships between the various elemental areas, and these may be obtained by combining the continuity equation with some simple geometric relations.

Suppose the surface S forming the back end of the control box is intersected by a plane N normal to the free stream, and consider the streamtube passing through a small rectangle $ABDC$ drawn in N , as in Fig. 4a. If this is sufficiently small, the streamlines through the circumference of the rectangle may be taken as parallel so that the streamtube intersects S in a parallelogram $BDEF$.

Then, in accordance with our definitions, dA_e is the area of the frontal projection of $BDEF$. This projection is shown in Fig. 4b, where an additional point M is constructed as shown. Also in this view we have dA_e^* shown as the area of $ABDC$, so that

$$\frac{dA_e^*}{dA_e} = \frac{AB}{MB}. \quad (12)$$

The right hand side of this equation may be evaluated by considering the plan view in Fig. 4c, and constructing the point L as shown. Then, since MB in Fig. 4b is equal to FL in Fig. 4c,

$$\frac{dA_e^*}{dA_e} = \frac{AB}{FL} = \frac{\cot \Lambda - \tan \varepsilon}{\cot \Lambda} \quad (13)$$

where $\tan \varepsilon = v_y/v_x$.

If ρ, v_x are respectively the density* and streamwise velocity component* at the point where the streamline crosses S , then continuity requires

$$\rho_\infty v_\infty dA_c = \rho v_x dA_e^* \quad (14)$$

so that by combining (12), (13) and (14) we obtain

$$\frac{dA_e}{dA_c} = \frac{\rho_\infty v_\infty}{\rho v_x} \frac{1}{1 - \tan \varepsilon \tan \Lambda} \quad (15)$$

or alternatively

$$\frac{dA_e}{dA_c} = \frac{\rho_\infty v_\infty}{\rho(v_x - v_y \tan \Lambda)}. \quad (16)$$

To find (dA_c/dA_p) suppose that at the point where the streamline intersects the shock wave, the normal to the shock surface has direction cosines (l, m, n) with respect to the co-ordinate system (x, y, z) ; then

$$\frac{dA_c}{dA_p} = \frac{l}{n}. \quad (17)$$

Inserting equations (14), (16) and (17) into (9) and (11), we have finally

$$f_L = \frac{2l}{n} \frac{v_x}{v_\infty} \quad (18)$$

$$f_D = \frac{2l}{n} \left[1 - \frac{v_x}{v_\infty} - \frac{(p - p_\infty)}{\rho v_\infty (v_x - v_y \tan \Lambda)} \right]. \quad (19)$$

*Throughout this Report, symbols describing flow variables, such as ρ, p, v_x, v_y, v_z , etc., will normally refer to conditions in the surface S . Free stream values will be distinguished by the suffix (∞) .

The foregoing derivations are, of course, quite arbitrary in many respects. It would have been possible to choose a different control volume, or a different method of associating elements of planform area with elements of force, and these alternative choices would be equally valid. Properly interpreted, all choices must lead to the same conclusions, but the present choice seems especially suitable, for the following reasons:

(a) Closing the control volume with a surface composed of vertical generators simplifies the algebra, since there are no pressure terms in the lift function.

(b) It also makes the planform area of the control volume identical with the planform area of the wing. This is convenient, since the first of these appears naturally in the algebra, and the second is an obvious choice as reference area.

(c) By arranging for the integrations to take place over the planform area, we give the lift and drag functions their useful 'mean value property' expressed by equations (8) and (10).

3. A Property of the Lift and Drag Functions.

By means of a simple example we shall now illustrate both the manner of use of the lift and drag functions, and a simple property of them.

Consider the flow past a two-dimensional double-wedge (Fig. 5a). Two regions of uniform flow may be recognised and designated (1) and (2) according to the number of shocks traversed. In any base plane BTT' the streamlines belong to one of two families, depending on whether they cross the initial shock AT upstream or downstream of the line SS' . Every streamline in the first family is associated with a particular value of the lift function, say, f_{L1} , and a particular value of the drag function, f_{D1} . Let the corresponding values for the second family be (f_{L2}, f_{D2}) .

Now draw lines AT, AT' in the initial shockwave and replace the streamsurfaces through them by a solid surface, as in Fig. 5b. Consider this to be the lower surface of a wing whose upper surface is stream-wise. Let us now use the methods of the previous Section to find the lift and drag of this wing. Referring to Fig. 5c we note that streamlines of type (1) are captured by a portion of the shockwave having planform area $ASS' (= A_1)$, and those of type (2) by a portion of the shockwave having planform area $S'T'TS (= A_2)$. From equations (8) and (10) we write at once:

$$C_L = \frac{A_1 f_{L1} + A_2 f_{L2}}{A_1 + A_2}, \quad (20)$$

$$C_D = \frac{A_1 f_{D1} + A_2 f_{D2}}{A_1 + A_2}. \quad (21)$$

Equations (20) and (21) express a simple property which may be illustrated as follows. Draw a set of rectangular axes (Fig. 6a) and label them f_L, f_D . Plot the point $P_1 (f_{L1}, f_{D1})$ which represents the first region of the flow field, and the point $P_2 (f_{L2}, f_{D2})$ which represents the second region. On the straight line $P_1 P_2$ find the point Q whose distance from P_1 is equal to $(P_1 P_2) (A_2)/(A_1 + A_2)$. Then equations (20) and (21) show that the co-ordinates of Q are (C_L, C_D) . It follows that, for any wing derived from the flow field under consideration, C_L and C_D are represented by the co-ordinates of some point lying between P_1 and P_2 , on the straight line joining them.

Now consider a general, three-dimensional flow field, in which each streamline defines a point (f_L, f_D) and suppose that all such points lie within some convex region* R of the (f_L, f_D) plane.

*A convex region is one whose boundary has no concave portions, so that the line joining any two interior points of R lies itself entirely within R .

To calculate C_L and C_D for a wing which captures a given part of this flow field, divide that part into a large number of small streamtubes, the n th streamtube being associated with lift and drag functions, f_{L_n} and f_{D_n} , and with an element of planform area ΔA_{p_n} . Then, for large enough n ,

$$C_L = \frac{\sum f_{L_n} \Delta A_{p_n}}{\sum \Delta A_{p_n}}$$

$$C_D = \frac{\sum f_{D_n} \Delta A_{p_n}}{\sum \Delta A_{p_n}}$$

(see Fig. 6b). To these expressions, any two small streamtubes will make, as in equations (20) and (21), an average contribution represented by some point within R . Subsequent addition of any number of streamtubes always leaves the net average contribution represented by a point within R , so that we may write the following theorem.

Theorem 1

If each streamline by the control volume of a lifting surface may be represented by a point lying within some convex region R of the (f_L, f_D) plane, then the point (C_L, C_D) representing the performance of the surface as a whole will also lie within R .

This theorem allows us to replace, to a certain extent, the task of seeking efficient wing shapes by the easier task of seeking flow fields containing efficient streamlines.

4. *Two-Dimensional Flow Fields.*

In this Section we shall apply the idea of lift and drag functions to some two-dimensional flows each with a single shock. For a two-dimensional flow we have $v_y = 0$, and $l/n = \tan \theta$, so that equations (18) and (19) assume the simpler form

$$f_L = 2 \tan \theta \frac{v_z}{v_\infty} \quad (22)$$

$$f_D = 2 \tan \theta \left[1 - \frac{v_x}{v_\infty} - \frac{(p - p_\infty)}{\rho v_x v_\infty} \right]. \quad (23)$$

4.1. *Flows Past Plane Wedges.*

Consider first the simplest case of flow at a given free stream Mach number past a plane wedge of semi-angle α . The lift and drag functions are both constant for all points on all streamlines. By use of the relationships derived in Appendix A for flow behind an oblique shock, equations (22) and (23) are easily reduced to:

$$f_{L_w} = C_p(\alpha) \quad (24)$$

$$f_{D_w} = C_p(\alpha) \tan \alpha$$

where $C_p(\alpha)$ is the pressure coefficient on the wedge.

Only the lower of the two possible values of C_p is valid.

As α changes at a given M_∞ , so equations (24) will define parametrically a curve in the lift-drag plane. This curve is concave upward for all Mach numbers and for all values of α having practical interest. It is shown diagrammatically as OS in Fig. 8.

For a given two-dimensional lifting wedge, or a given Nonweiler wing, f_L and f_D are constant, and equations (8) and (10) give

$$C_L = f_L$$

$$C_D = f_D.$$

Thus the curve OS has a dual interpretation, representing either the lift and drag functions of streamlines in a wedge flow, or the lift and drag coefficients of the bodies themselves. Its equation may be explicit by manipulating the oblique shock relationships to obtain

$$f_{Dw} = \frac{f_L^2}{2-f_L} \left[\frac{1 - \frac{1}{M_\infty^2} - \frac{\gamma+1}{4} f_L}{\frac{1}{M_\infty^2} + \frac{\gamma+1}{4} f_L} \right]^{\frac{1}{2}} \quad (25a)$$

Here f_{Dw} is the drag function of a streamline which achieves a given lift function f_L by being deflected through a plane shockwave.

Alternatively, we may write

$$C_{Dw} = \frac{C_L^2}{2-C_L} \left[\frac{1 - \frac{1}{M_\infty^2} - \frac{\gamma+1}{4} C_L}{\frac{1}{M_\infty^2} + \frac{\gamma+1}{4} C_L} \right]^{\frac{1}{2}} \quad (25b)$$

where C_{Dw} is the drag coefficient of a plane wedge which produces a given lift coefficient C_L .

In assessing the performance of any given wing, equation (25b) affords a useful standard of comparison. If a given wing has force coefficients C_L , C_D , we may form an 'efficiency ratio', E_w , by comparing its performance with a wedge developing the same C_L , i.e.

$$E_w = \frac{(L/D)}{(L/D)_w} = \frac{C_{Dw}}{C_D} \quad (26)$$

The evidence to date suggests that the maximum value of E_w attainable by practical wing shapes with attached shock waves and unswept trailing edges is about 1.1.

In a similar way, we may use equation (25a) to assess the 'performances' of various streamlines, defining

$$E_s = \frac{f_{Dw}}{f_L} \quad (27)$$

4.2. Optimum Two-Dimensional Flow Fields.

Consider a two-dimensional flow with a single shock wave, as in Fig. 7. To compute such flows we shall, for simplicity, use shock-expansion theory to calculate the flow properties, which will then depend only on the local flow inclination, and the strength of the part of the shock through which that flow has passed. Thus, for given free-stream conditions, the entropy level along any given streamline is known from the appropriate shock strength, and knowledge of any additional flow property will enable us to calculate all the others. There is, therefore, a unique relationship between the lift and drag functions, along a specified streamline or any other streamline at the same entropy level. Moreover, the curve in the lift-drag plane (see Fig. 8) which expresses this relationship must, when it corresponds to conditions at P , just behind the shock wave, intersect or touch the plane shock curve given by equation (25a). It may be shown that the part of the curve lying to the right of P represents an isentropic compression after the shock; the part to the left represents an expansion.

We shall now look for streamlines which are 'optimum' in the sense of producing least f_D for a given f_L . To do this, suppose that for all points such as P on OS in Fig. 8 the curve corresponding to PQ has been drawn (Fig. 9). The envelope of these curves (OE) evidently indicates the minimum value of f_D attainable for any given f_L , and any point Q on the envelope determines unique values of shock strength* and isentropic turning angle.

*Each curve PQ crosses OS twice, but only at one of these points are the oblique shock equations satisfied. The other point is of no special significance.

The equations which are satisfied on OE are extremely complex; here therefore a cruder but very much simpler approach has been taken. A computer programme has been written which traces points on the curves PQR along such arcs as lie below OS . For any given free stream Mach number the programme computes between eight and sixteen points on each of a number of arcs. The envelope is then found graphically.

It is, therefore, possible to represent any streamline in a two-dimensional flow having only one shock wave by a point lying within the region of Fig. 9 bounded by OQE , and the vertical axis. Since calculations show this region to be convex, it follows from Theorem 1 in Section 3 that the performance (C_L, C_D) of any wing supporting a two-dimensional flow field is also represented by a point within this region. It is impossible, therefore, to find better wings than those whose representations actually lie on the boundary OQE . If such a wing can be constructed, all the streamlines it captures will have identical lift and drag functions, as for example the two-dimensional wing shown in Fig. 10a. If all these streamlines are represented by, say, the point Q in Fig. 9, then

$$f_L = \text{const} = f_{LQ} = C_L$$

$$f_D = \text{const} = f_{DQ} = C_D.$$

Both the shock strength and the final deflection are uniquely determined by Q . Thus the flow field consists of a constant-strength shock wave OS , followed by an isentropic compression centered on S . In fact, the calculations show that the angle $(\delta - \delta_1)$ is usually small, and it is sufficiently accurate to take as the optimum wing a double wedge with the same initial and final deflections. In that case the flow will contain a weak second shock wave, but this has a negligible effect upon the calculations.

At low Mach numbers ($1 < M_\infty < 2.5$) it turns out that the optimum streamlines are expanded rather than compressed behind the initial shock. It is not then possible to make all the streamlines captured by a wing identical (see Fig. 10b), but the error incurred by assuming them to be identical for an optimum wing is very small.

Some computed results for the optimum surfaces are shown in Figs. 11 and 12. Fig. 11 shows the performance of optimum surfaces, having given values of C_L at given Mach numbers, in terms of the efficiency ratio E_w defined in equation (26). It will be observed that the extent to which E_w can be raised above unity is very small, amounting in all cases shown to a fraction of one per cent.

These results are similar to those of Pike⁷, who has investigated the problem of optimum two-dimensional lifting surfaces by means of a theory which goes beyond shock-expansion theory by taking into account, to first order, the disturbances reflected from the shock wave. He also finds a double wedge to be the optimum shape, but folded further forward, and his maximum values of $(E_w - 1)$ are some 50 per cent greater than those shown here. The interested reader may compare these results with those of Bartlett⁸, who investigates double wedges enclosing a given volume, and finds that the lift-drag ratios are higher for convex shapes.

In Fig. 12 the ratio of final to initial deflection is plotted for the optimum surfaces. Note that at high Mach numbers the shape is concave, whereas at low Mach numbers it is slightly convex. This statement is also in agreement with Pike's results⁷.

5. Flow in a Plane of Symmetry.

5.1. Statement of the Problem.

We shall now extend the analysis of optimum streamlines, given for two-dimensional flow in the previous Section, to more general flows having a plane of symmetry. This case is important because (a) almost all practical lifting shapes possess at least one such plane, (b) the widest class of flow fields which are readily calculable at the present time are axisymmetric, and have infinitely many planes of symmetry.

If we restrict our attention to flow in a vertical plane of symmetry we have again $v_y = 0$, $l/n = \tan \theta$ so that the expressions for the lift and drag functions are precisely as in two-dimensional flow :

$$f_L = 2 \tan \theta \frac{v_z}{v_\infty} \quad (22)$$

$$f_D = 2 \tan \theta \left[1 - \frac{v_x}{v_\infty} - \frac{(p - p_\infty)}{\rho v_x v_\infty} \right]. \quad (23)$$

The vital difference between the two cases is that, because the air on either side of the plane of symmetry can now be expanded or compressed sideways, there is no longer even an approximate relationship between flow direction and pressure coefficient say, or any other flow variable. For example, on the surface of an elliptic cone, at a point in one of the planes of symmetry, the pressure can be made to assume a wide range of values by changing the eccentricity of the ellipse, even though the surface may make the same angle with the free stream in every case. Thus, at any given deflection, a very wide range of pressures can be achieved in different flow fields.

At the beginning of the analysis it will be assumed that this range is unlimited, i.e. any direction and any pressure may be combined at some point in some flow. However, pressures, velocities and densities are not all independent, since the equations of one-dimensional gas dynamics must be satisfied along streamlines. This is sufficient to put some restraint on the values which the lift and drag functions may assume, and we shall find, as in the previous Section, an envelope which contains all the possible values and hence defines optimum streamlines. An *a posteriori* justification of this procedure is provided by the fact that streamlines having very nearly the calculated optimum properties are in fact found in computed flow fields.

5.2. Optimum Streamlines Behind a Given Shockwave.

In this Section we consider the possible values of the lift and drag functions which may arise along a streamline which lies in a plane of symmetry and passes through an initial shock wave of given strength. We allow the possibility that the streamline subsequently passes through additional shock waves. The object of this Section is to prove the following theorem.

Theorem 2.

Of all streamlines in the class defined above and producing given values of f_L , those which give rise to the smallest values of f_D are those which, after passing through the initial, given, shock wave, are isentropically expanded back to free-stream pressure.

To show this we begin by expressing the lift and drag functions in terms of the fewest possible number of independent variables, i.e. four*, and choose these to be as follows :

- (a) θ , the inclination of the given shock wave,
- (b) Δs , the specific entropy rise,
- (c) \bar{v} , the ratio of local velocity to the maximum velocity attainable by expansion into a vacuum, i.e. v/v_{\max} , (note that v_{\max} does not change across shock waves), and
- (d) δ , the local flow deflection relative to the free-stream.

Defining

$$\lambda = e^{-\frac{\Delta s}{R}} = \frac{\rho_t}{\rho_{t_\infty}} = \frac{p_t}{p_{t_\infty}}$$

*The free-stream Mach number is taken as a constant in any particular problem. It does not suffice together with θ to determine Δs , as the streamline may pass through more than one shock.

and substituting standard gasdynamic relationships into equations (22) and (23) we obtain

$$f_L = 2 \tan \theta \frac{\bar{v} \sin \delta}{\bar{v}_\infty} \quad (28)$$

$$f_D = 2 \tan \theta \left[1 - \frac{\bar{v} \cos \delta}{\bar{v}_\infty} - \frac{k(\bar{v})}{\cos \delta} \right] \quad (29)$$

where

$$k(\bar{v}) = \frac{1}{\gamma M_\infty^2} \left[\frac{1 - \bar{v}^2}{1 - \bar{v}_\infty^2} - \frac{1}{\lambda} \left(\frac{1 - \bar{v}_\infty^2}{1 - \bar{v}^2} \right)^{\frac{1}{\gamma-1}} \right] \frac{\bar{v}_\infty}{\bar{v}} \quad (30)$$

and k has the same sign as $(p - p_\infty)$.

Consider now the class of streamlines, which after passing through the initial shock wave, reach given values of \bar{v} and δ , but some of which pass through 'embedded' shock waves, and so have various entropy levels. The flow fields which contain these different streamlines may be supposed to be generated by bodies of suitably chosen cross-section shapes and longitudinal area distributions. All the streamlines so defined have the same value of f_L (see equation (28)), but differing values of f_D . We now choose λ so as to minimise f_D . Inspection of equations (29) and (30) shows that this is achieved by setting λ as large as possible. Since each shock wave in the flow reduces the value of λ , the lowest value of f_D is reached by eliminating all shock waves except the initial, given, one. In this case λ is given by

$$\lambda = \left[\frac{(\gamma+1) M_\infty^2 \sin^2 \theta}{(\gamma-1) M_\infty^2 \sin^2 \theta + 2} \right]^{\frac{1}{\gamma-1}} \left[\frac{\gamma+1}{2\gamma M_\infty^2 \sin^2 \theta - (\gamma-1)} \right]^{\frac{1}{\gamma-1}}. \quad (31)$$

In all subsequent analysis it will be assumed that the flow is isentropic behind the initial shock, so that equation (31) holds.

Now suppose that, in equations (28) and (29), δ remains fixed whilst \bar{v} varies through all possible values up to unity. Then the point (f_L, f_D) will trace out some locus in the lift-drag plane (see Fig. 13). For various values of δ , a family of loci will thus be obtained whose outer envelope will represent the maximum possible efficiency of streamlines passing through an initial shock of inclination θ . Such an envelope can be clearly seen in Fig. 13.

The formal expression for this envelope is (Ref. 9 p174)

$$\frac{\partial f_L}{\partial \bar{v}} \cdot \frac{\partial f_D}{\partial \delta} - \frac{\partial f_L}{\partial \delta} \cdot \frac{\partial f_D}{\partial \bar{v}} = 0$$

and applying this to equations (28) and (29) gives, as a relationship between \bar{v} and δ along the envelope

$$k \tan^2 \delta = \frac{\bar{v}}{\bar{v}_\infty} + \bar{v} \frac{dk}{d\bar{v}} \quad (32)$$

where $dk/d\bar{v}$ is obtained from equation (30) as

$$\frac{dk}{d\bar{v}} = \frac{-1}{\gamma M_\infty^2} \frac{\bar{v}_\infty}{\bar{v}^2} \left[\frac{1 + \bar{v}^2}{1 - \bar{v}_\infty^2} + \frac{\left\{ \left(\frac{\gamma+1}{\gamma-1} \right) \bar{v}^2 - 1 \right\} \left(1 - \bar{v}_\infty^2 \right)^{\frac{1}{\gamma-1}}}{\lambda (1 - \bar{v}^2)^{\frac{1}{\gamma-1}}} \right]. \quad (33)$$

Now when $k = 0$, i.e. when $p = p_\infty$, we can obtain from equation (30),

$$\frac{1 - \bar{v}_0^2}{1 - \bar{v}_\infty^2} = \frac{1}{\lambda} \left(\frac{1 - \bar{v}_\infty^2}{1 - \bar{v}_0^2} \right)^{\frac{1}{\gamma-1}} \quad (34)$$

in which \bar{v}_0 is the value of \bar{v} which makes $p = p_\infty$. If this relationship is substituted into equation (33) and use made of the identity,

$$M_\infty^2 = \frac{2}{(\gamma-1)} \frac{\bar{v}_\infty^2}{1 - \bar{v}_\infty^2},$$

it is easily shown that, when $p = p_\infty$, both sides of equation (32) vanish, so that the condition $p = p_\infty$, i.e. $\bar{v} = \bar{v}_0$, defines the envelope we are looking for. This completes the proof of theorem 2.

It is perhaps appropriate to recall here that on bodies of revolution, zero pressure coefficients are usually reached when the body slope is still sizeably positive. Thus we may have confidence that the 'optimum streamlines', may be found in real physical flows. The example given later in Section 6.3 is of interest in this connection.

When $p = p_\infty$ the expressions for f_L and f_D are as follows:

$$\left. \begin{aligned} f_L &= 2 \tan \theta \frac{\bar{v}_0 \sin \delta}{\bar{v}_\infty} \\ f_D &= 2 \tan \theta \left[1 - \frac{\bar{v}_0 \cos \delta}{\bar{v}_\infty} \right] \end{aligned} \right\} \quad (35)$$

These equations represent a circle, of radius $2 \tan \theta (\bar{v}_0/\bar{v}_\infty)$, with its centre at $f_L = 0, f_D = 2 \tan \theta$. It is given explicitly by

$$f_L^2 + (f_{D_{\min}} - 2 \tan \theta)^2 = 4 \tan^2 \theta \frac{\bar{v}_0^2}{\bar{v}_\infty^2}.$$

For small deflection angles and weak shock waves we may make the approximations $\bar{v}_0 = \bar{v}_\infty$, $\tan \theta = (M_\infty^2 - 1)^{-\frac{1}{2}} = 1/\beta$, and neglect f_D^2 , to obtain

$$f_{D_{\min}} \simeq \frac{1}{4} \beta f_L^2. \quad (36)$$

In the flow past a two-dimensional wedge at a small angles to the free-stream, we have, e.g. by simplifying equations (25a)

$$f_{D_w} \simeq \frac{1}{2} \beta f_L^2 \quad (37)$$

so that, for small deflections, optimum streamlines give rise to just half the drag of streamlines which produce the same lift in a plane wedge flow. Alternatively, we may say that optimum streamlines in a plane of symmetry in a three-dimensional flow are twice as efficient as optimum streamlines in a two-dimensional flow.

5.3. Optimum Shock Strength.

There is still a further stage of optimisation to be undertaken. The results of Section 5.2 assumed that the initial shock strength was given. By relaxing this condition, but still making use of the results of Section 5.2, we shall be able to show the following result.

Theorem 3

Of all streamlines possible in a plane of symmetry, which produce given finite values of f_L , those which give rise to the smallest values of f_D pass through an initial shock wave of finite strength.

At any given free-stream Mach number, Section 5.2 shows that each possible choice of initial shock strength gives rise, *via* equation (35), to a family of optimum streamlines described by a circular locus in the lift-drag plane. These circles themselves have an envelope, which defines absolutely optimum streamlines for that Mach number, as shown in Fig. 14.

Its equation may be written⁹

$$\frac{\partial f_L}{\partial \delta} \cdot \frac{\partial f_D}{\partial \theta} - \frac{\partial f_D}{\partial \delta} \cdot \frac{\partial f_L}{\partial \theta} = 0.$$

Substituting in this from equations (35) we have

$$\cos \delta = \frac{\bar{v}_0}{\bar{v}_\infty} + \frac{\cos \theta \sin \theta}{\bar{v}_\infty} \frac{d\bar{v}_0}{d\theta}. \quad (38)$$

To evaluate this expression, combine equations (31) and (34) to give

$$1 - \bar{v}_0^2 = (1 - \bar{v}_\infty^2) \left[\frac{(\gamma - 1) M_\infty^2 \sin^2 \theta + 2}{(\gamma + 1) M_\infty^2 \sin^2 \theta} \right] \left[\frac{2\gamma M_\infty^2 \sin^2 \theta - (\gamma - 1)}{(\gamma + 1)} \right]^{\frac{1}{\gamma}} \quad (39)$$

If this is differentiated with respect to θ and the result substituted into (38) there is obtained

$$\cos \delta = \frac{\bar{v}_0}{\bar{v}_\infty} - \frac{4 \cos^2 \theta}{(\gamma + 1)^2 M_\infty^2} \frac{\bar{v}_0}{\bar{v}_\infty} \frac{(M_\infty^2 \sin^2 \theta - 1)^2}{M_\infty^2 \sin^2 \theta} \left[\frac{(\gamma + 1)}{2\gamma M_\infty^2 \sin^2 \theta - (\gamma - 1)} \right]^{\frac{1}{\gamma-1}} \quad (40)$$

Equations (39) and (40), together with equation (35) enable the envelopes to be calculated in terms of the parameter θ .

For weak shock waves a much simpler relationship can be obtained by expanding equation (40) as a power series, thus:

$$\cos \delta = 1 - \frac{4(M_\infty^2 - 1)}{(\gamma + 1)^2 M_\infty^4} (M_\infty^2 \sin^2 \theta - 1)^2 + 0 (M_\infty^2 \sin^2 \theta - 1)^3. \quad (41)$$

Since $\cos \delta$ is roughly $1 - \delta^2/2$, we have

$$\delta_{\text{OPT}} \approx \frac{2\sqrt{2}(M_\infty^2 - 1)^{\frac{1}{2}}}{(\gamma + 1) M_\infty^2} (M_\infty^2 \sin^2 \theta - 1). \quad (42)$$

Now from the oblique shock relationships, if δ_1 is the (small) deflection immediately behind the shock

$$\delta_1 \approx \frac{2(M_\infty^2 - 1)^{\frac{1}{2}}}{(\gamma + 1) M_\infty^2} (M_\infty^2 \sin^2 \theta - 1) \quad (43)$$

whence

$$\delta_{\text{OPT}} \approx \sqrt{2} \delta_1. \quad (44)$$

The results of exact calculations, using equations (34), (39) and (40) are presented in Figs. 15 and 16, the comparison being made at equal values of f_L . It will be noted from Fig. 15 that the optimum flow process is between 50 and 100 per cent more efficient than the plane shock process.

5.4. Discussion.

The results so far obtained in this Section have indicated the properties possessed by optimum streamlines lying in a plane of symmetry. We cannot, unfortunately, use these to discover optimum flow fields in the same way that we did for two-dimensional flows, because it will not be possible to construct the flow field out of identical streamlines. However, the optimum properties do give a strong indication of the properties which will be desirable in real flows.

For example, the fact that the optimum flow processes return the air to free-stream pressure makes it a plausible assumption that high efficiency will generally be associated with low pressure coefficients at the point where the streamline leaves the control volume. This assumption is borne out by all the calculations made to date, although the efficiency appears to fall off quite rapidly if negative pressure coefficients are encountered.

The fact that there exists for any given lift coefficient an optimum shock strength different from zero may be found a little surprising, but there is in fact a simple physical explanation. Steeper shock waves are associated with larger entropy rises and hence higher drag (*see* equations (29) and (30) *et seq.*) but they also 'capture' more air per unit planform area. This is expressed by the term $\tan \theta$ in the expressions for f_L and f_D . For weak shocks the second of these two effects is the more important. The result is of considerable practical significance as showing that the presence of finite initial shock waves may be beneficial provided they are not too strong. However, this applies only to the initial shock wave; any subsequent shock 'embedded' in the flow does not cause a loss of efficiency, since the additional entropy rise is not compensated by any gain in (capture area)/(planform area).

6. Some Miscellaneous Applications.

In Sections 4 and 5 we were able to derive qualitative results by making certain symmetry assumptions. In this Section we shall use the lift and drag functions to indicate a number of results which are more general, but less precise.

6.1. Wings with Unswept Trailing Edges Supporting Flow Fields with Axial Symmetry.

6.1.1. *Basic equations.* Consider a wing derived by freezing a streamsurface in the flow past an axisymmetric body (Fig. 17). Any streamline PQ captured by the wing lies in an axial plane. Suppose this plane to make an angle ψ with the vertical. Then for such a streamline we have:

$$\left. \begin{aligned} v_y &= v_r \sin \psi \\ v_z &= v_r \cos \psi \\ l/n &= \tan \theta / \cos \psi \end{aligned} \right\} \quad (45)$$

and if the wing has an unswept trailing edge $\Lambda \equiv 0$.

Substituting these results in equations (18) and (19) we obtain for the lift and drag functions

$$f_L = 2 \tan \theta \frac{v_r}{v_\infty} \quad (46a)$$

$$f_D = \frac{2 \tan \theta}{\cos \psi} \left[1 - \frac{v_x}{v_\infty} - \frac{(p - p_\infty)}{\rho v_x v_\infty} \right]. \quad (46b)$$

6.1.2. *Variation of lift and drag functions away from central plane.* The streamline which leaves the control volume through the point (x_B, r, ψ) will be associated with particular values of the lift and drag functions. Denote these by $f_L(r, \psi), f_D(r, \psi)$.

Since the flow is axially symmetric equations (46) give at once

$$\left. \begin{aligned} f_L(r, \psi) &= f_L(r, 0) \\ f_D(r, \psi) &= f_D(r, 0) \sec \psi \end{aligned} \right\} \quad (47)$$

Thus the lift contributed by an elementary streamtube depends only on its radial position, but the drag increases away from the central plane ($\psi = 0$), so that *the most efficient parts of the flow field are those closest to this plane*. The implications of this statement will be considered in Section 6.2.

The flow in any plane of symmetry $\psi = \text{const}$ may be analysed as in Section 5, all the results of which hold here, except that all drag functions are multiplied by $\sec \psi$. In particular the optimisation processes are still valid, so the same type of flow is desirable; that is, initial deflection through a weak finite shock-wave, no subsequent shocks, and expansion to conditions of small pressure coefficients, but positive deflection, in the plane $x = x_b$.

6.1.3. *Relationship between lift and flow deflection.* Equation (46a) may be rewritten

$$f_L = 2 \tan \theta \left(\frac{v}{v_\infty} \right) \sin \delta \quad (48)$$

where δ is the flow deflection angle. Of the terms in this equation, $\tan \theta$ will probably be almost constant for a given shockwave, and slightly greater than $1/\beta_\infty$ everywhere, whereas (v/v_∞) will be a little less than unity, so that the lift function is very nearly proportional to $\sin \delta$, and, for a given Mach number, far less influenced by any other variable. By recalling the basic result, equation (8), that the lift coefficient is a mean value of the lift function, we see that a good estimate of the lift coefficient developed by any wing chosen to support an axisymmetric flow field is provided by a knowledge of the average flow deflection in the captured part of the field. Note that it is the deflection relative to the axis (v_r/v) rather than the vertical component (v_z/v) of this deflection which is involved.

This simple relationship is useful if it is desired to construct a surface of given lift coefficient, and the problem is to choose an appropriate flow field.

6.1.4. *References to other work.* For the special case of the flow field about an unyawed circular cone, Woods¹¹ has presented single integral formulae for the lift, drag, pitching moment, and planform area of a derived lifting surface. His formulae, are also derived by a momentum analysis, although based on a slightly different control volume.

Another example of momentum analysis which, although not so relevant to the present work, affords some interesting points of comparison, is that given by Zandbergen¹². He is interested in bodies of revolution having minimum pressure drag within exact inviscid theory, although mathematical difficulties limit him to consideration of bodies supporting homentropic flow fields, as in Fig. 18. His optimum solutions, like those of the present work, incorporate a finite initial shockwave.

6.2. 'Mapping' of Flow Fields.

Consider a surface S composed solely of vertical generators, and situated in a known flow field F , so that streamlines of F pass through S . Consider the class C of lifting surfaces which are streamsurfaces of F , and whose trailing edges lie in S . Given F and S , we can compute lift and drag functions for all the streamlines captured by any member of C and hence find C_L and C_D . In this Section it will be shown how a 'map' of the lift and drag functions may assist in choosing efficient members of C .

To illustrate the method we shall take F to be one of the homentropic flow fields recently calculated by Moore¹⁰, who has computed the flow past various bodies of revolution. A typical flow is illustrated in Fig. 18. The body of revolution to be considered is generated by OCB . The front portion OC , ($0 < x < x_c$), is a cone, which produces a conical flow field bounded by the shockwave OT and the characteristic CT . This part of the flow is taken from calculations by Bartlett¹³. The remainder of the body, CB , is defined by some simple analytic function $r = r(x)$, and the flow in the region CTB is calculated by the method of

axisymmetric characteristics. In the particular example chosen, the angle CON is 8° , and the curve CB is defined by

$$\left(\frac{r}{x_c}\right) = -0.015 \left(\frac{x}{x_c}\right)^2 + 0.170541 \left(\frac{x}{x_c}\right) - 0.015.$$

The Mach number in the free-stream is 3.0.

For simplicity we shall consider only wings with unswept trailing edges, and accordingly choose the surface S to be one of the planes $x = \text{constant}$. Here we choose arbitrarily the plane $\left(\frac{x}{x_c}\right) = 5.0$ which lies just in front of the plane TBN . To achieve maximum efficiency one should attempt to find a flow field and a trailing edge plane such that the recommendations of Sections 6.1.2 and 6.1.3 are met, that is, an average flow deflection related to the required lift coefficient by equation (48), together with as low an overall pressure coefficient as possible. This requirement is rather vague, but definite enough to be of use in what would otherwise be a purely trial and error process. Here, as the objective is merely to illustrate the mapping technique, no particular effort has been made to optimise the choice of flow field or trailing edge plane.

The technique is to associate with each point on the shockwave the values of f_L and f_D corresponding to the streamline through that point. Then contour maps may be drawn in the surface of the shockwave representing lines of constant f_L or constant f_D . When such a map is seen in plan view (Fig. 19), the lift and drag coefficients of a wing capturing any part of the flow field are, by equation (8), the mean values of f_L and f_D over the planform area of the wing. Inspection of such a map may be helpful in determining which regions of the flow field should be captured by the lifting surface.

A slightly different map which may also be of use is shown in Fig. 20. Here the function plotted is the 'efficiency ratio' E_s defined by equation (27).

It is shown in Fig. 20 for each streamline as it emerges from the trailing edge plane. Although there is now no simple general relationship between the efficiencies shown and the efficiency of a wing derived from the flow, some broad features of the flow are very clearly apparent. Several of these are common to all axisymmetric flow fields, and are as follows:

- (a) $E_s = 0$ along $\psi = \pm \pi/2$,
- (b) $E_s = \cos \psi$ along the shock wave,
- (c) The curve $E_s = 1$ touches the shock wave at $\psi = 0$,
- (d) The region $E_s > 1$ lies inside the curve $E_s = 1$.

Note that in the present example a local value of $E_s = 1.95$ has been achieved at one point in the flow. This is very close to the optimum values calculated in Section 5.

Although, as has been said, no particular effort was made to optimise the flow field on which Fig. 20 was based, experience so far indicates that it may be considered representative of fairly efficient axisymmetric flows. By way of contrast, Fig. 21 is offered as an example of a badly chosen flow field. The flow is about a 10° cone-cylinder at $M_\infty = 4.0$, for which the basic data are given in Ref. 14. The trailing edge plane has been chosen to coincide with the plane in which the characteristic from the shoulder intersects the shock wave, i.e. $x/x_c = 2.63$. There is an annular region around the body in which the flow is overexpanded and directed slightly inward, so that in this region f_L is small and negative. As a convenient convention E_s has been shown as negative also.

It should be emphasised that the maps described in this Section do not refer to flow fields by themselves, but to the combination (flow field) + (trailing edge surface).

The idea of drawing maps in the trailing edge surface was suggested to the author by J. Pike of the Royal Aircraft Establishment, Bedford.

6.3. On Different Types of Flow Field.

We begin by comparing axisymmetric and two-dimensional flow fields. Consider two streamlines in an axisymmetric flow, and let them lie in meridian planes separated by a small angle $\Delta\psi$. Also let the two streamlines be at the same radial position. Then as the streamlines move away from the axis they diverge, and when moving toward the axis they converge. (In a two-dimensional flow they would remain equidistant.) These considerations help to explain the well-known fact that a given body profile gives lower surface pressures at corresponding points when it is used to generate a body of revolution than when it is used to generate a two-dimensional body (see Fig. 22). The converse is true if the same profile is used to generate the inside of an axisymmetric duct; here surface pressure will be higher than on the two-dimensional body.

Now in Section 6.1.3. we have seen that lift is associated with flow deflection, and in Section 6.1.1. that low drag is associated with small static pressure. It is reasonable to expect, therefore, that efficient streamlines are more likely to be found in external axisymmetric flows than in two-dimensional flows, and less likely to be found in internal axisymmetric flows. All the examples available to date confirm this expectation, and some typical numerical evidence is presented in Fig. 23. This compares the properties of four flow fields, each associated with the flow at $M_\infty = 6.0$ into a constant-strength shock wave of inclination $\theta = 20^\circ$; these flows are

- (i) The flow past a right circular cone, of semi-apex angle 16.00° .
- (ii) The flow through a particular axisymmetric duct, whose intake is shaped¹⁵ so as to support a reversed conical shock wave.
- (iii) The flow past a two-dimensional wedge of semi-angle 12.44° , followed by an isentropic compression.
- (iv) The flow past a two-dimensional wedge of semi-angle 12.44° , followed by an isentropic expansion.

Flow fields (i) and (ii) have constant properties along conical rays; flow fields (iii) and (iv) have constant properties along outgoing characteristics (at least within shock-expansion theory). For each of the four cases, therefore, there is a unique relationship between f_L and f_D , provided we consider only the vertical plane of symmetry. These relationships are shown, in terms of the 'efficiency ratio', in the four curves illustrated in Fig. 23. Clearly the most efficient streamlines are those in the external axisymmetric flow, even though the shock wave is followed by a compression, rather than an expansion which would be more in line with the recommendations of Section 5. When an external axisymmetric shock wave is correctly followed by an expansion, as in the example given in Fig. 20 and described in Section 6.2, much more efficient streamlines are achieved, and efficiency ratios close to the optimum values calculated in Section 5 are encountered.

These are only to be found, however, in the central plane $\psi = 0$. On either side of this the efficiency falls away, as we have seen, in proportion to $\cos \psi$.

It would be possible to construct a very efficient wing which captured only the central part of the flow field shown in Figs. 19 and 20. Such a wing in fact has a very sharply anhedralled undersurface, however, and would suffer from, amongst other disadvantages, a large friction drag. If a flatter, more realistic, wing shape is to capture, and take advantage of, the more efficient parts of the flow field, it must necessarily capture some of the less efficient regions as well.

This situation is inescapable with axisymmetric flow fields; the efficient streamlines attainable in the central plane are bought at the price of less efficient streamlines elsewhere. By contrast, the streamlines in the central plane of a wing supporting a two-dimensional flow are more limited in their possible efficiency, but the streamlines do not, of course, deteriorate in efficiency outside this plane. These considerations suggest that the best flow fields for practical use might well be, in some sense, intermediate between two-dimensional and axisymmetric. Such flow fields might be generated, for instance, by bodies of elliptic cross section, or by bodies of revolution at small angles of attack. These flows, however, have only been calculated to date in the special case of conical flow.

6.4. Effects of Trailing-Edge Sweep.

So far in this Report, attention has been concentrated on wings with unswept trailing edges. In fact, the algebra is so much complicated by allowing the trailing edge to be swept that very few simple analytical results can then be obtained. One of these few is demonstrated in Appendix C, which shows the relationship between trailing edge sweep and efficiency for a double Nonweiler wing². This particular result, however, could equally well have been derived geometrically.

Nevertheless, some qualitative conclusions can be obtained from inspection of the basic equations (18) and (19), which are repeated below for convenience.

$$f_L = \frac{2l}{n} \frac{v_z}{v_\infty} \quad (18)$$

$$f_D = \frac{2l}{n} \left[1 - \frac{v_x}{v_\infty} - \frac{p - p_\infty}{\rho v_\infty (v_x - v_y \tan \Lambda)} \right]. \quad (19)$$

First of all note that the spanwise velocity component v_y and the trailing edge sweep Λ occur only in the combination $(v_y \tan \Lambda)$ and that the efficiency of the streamtube is enhanced by increasing the value of this parameter (provided $p > p_\infty$). If we suppose a given flow field to have symmetry about the x_z plane, and v_y directed everywhere away from this plane (e.g. the flow past a cone) then the local efficiency of any streamline will be improved by making Λ positive*, that is, by sweeping the trailing edge back.

Alternatively if v_y is directed toward the plane of symmetry, as for example in the flow field associated with axisymmetric converging duct¹⁵ discussed in the last Section, a gain of efficiency will result from sweeping the trailing edge forward.

Let us apply these ideas to the flow field about a flat-plate delta wing. Below the wing we have $p > p_\infty$ and v_y directed outward; above the wing $p < p_\infty$ and v_y directed inward. It may be concluded that the efficiency of both the upper and lower surface flows will be improved if the trailing edge is swept back. This result is in accordance with well known facts about the performance of arrow-head wings.

6.5. A Possible Experimental Application.

The preceding Sections of this Report have attempted to define the type of flow process that generates lift efficiently. To summarise once again, the desirable features of a lifting flow field are;

- (a) Finite but weak initial shockwave,
- (b) No embedded shocks,
- (c) At the rear end of the control volume;
 - (i) Low pressure coefficients,
 - (ii) Large vertical velocity components,
 - (iii) Small spanwise velocity components, except in the case of a swept trailing edge, when equation (C-3) gives a rough indication of the desirable spanwise deflection.

It is possible that further work might refine and quantify the above remarks, but even as they stand they might be made the basis of an experimental technique to design efficient lifting shapes along the following lines.

Suppose that some empirically designed shape, meeting certain requirements on planform and volume, can be tested at its intended lift coefficient in a wing tunnel. Schlieren observations can be made to measure the strength of the initial shockwave, and to detect any embedded shocks. A flow survey below the trailing

*Evidently Λ cannot be increased beyond the point at which the trailing edge becomes sonic without invalidating the present method of analysis.

edge can be made to measure pressures and flow directions there. If any parts of the flow field do not meet the above requirements, it may be possible to tailor the original shape so as to alleviate the extent to which they depart from optimum flow processes, and thereby to enhance the efficiency of the shape.

7. Future Work.

The type of analysis introduced in this Report could be extended to cover the case of lifting flows with heat addition, and might consider the relative merits of the following schemes :

- (a) Instantaneous heat addition at the initial shockwave.
- (b) Instantaneous heat addition at an embedded shockwave.
- (c) Heat addition distributed over a finite length of the flow.

(d) Heat addition to various selected regions of an axisymmetric flow, that is to say, near the tips, or near the centre. Mr. L. H. Townend has suggested, in a private communication, that the most efficient layout is to be achieved by placing engines near the tips. He argues that the thrust provided by a given engine should be independent of its angular position in the flow field, so that for good overall performance it will be best placed in those parts of the flow field which are of low lifting efficiency.

8. Conclusions.

A relationship has been derived between lift and drag produced in inviscid flow by a surface with attached shockwaves, and the changes in pressure and momentum produced along nearby streamlines. On this basis lift and drag functions are associated with each streamline. These are such that the lift and drag coefficients of a wing are mean values of the corresponding functions for those streamlines which are 'captured'. Use of these functions enables the generation of lift to be studied in terms of the flow processes involved.

An analysis of two-dimensional flow fields, into which shock-expansion theory is introduced as a simplifying assumption, allows optimal flow fields to be found; these indicate that the optimum lifting shapes are very close to double wedges in shape, and have performances only fractionally superior to plane wedges.

The analysis is then extended to flow in a plane of symmetry, when, without any simplifying assumptions except those involved in the dynamics of a perfect gas, it is found possible to compute optimum flow processes. These have the following main features.

- (a) The air is initially deflected by passing through a weak, but finite shockwave.
- (b) All subsequent flow processes are purely isentropic.
- (c) The air is expanded so as to be at free-stream static pressure as it passes out of the control volume.
- (d) The final deflection is $\sqrt{2}$ times the initial deflection, if these are both small.
- (e) If only small perturbations of the free-stream are involved, the lifting efficiency of the optimum process is twice that of a flow which produces the same lift by means of a plane shock.

These optimum processes are used to suggest desirable features of flow processes in more general situations. Particular attention is given to the case of a wing obtained by 'freezing' a streamsurface in an axisymmetric flow field. In such a field it is possible to create regions of much higher lifting efficiency than can be achieved in a two-dimensional field; other regions, however, are necessarily of lower efficiency.

The effect on efficiency of trailing edge sweep is considered qualitatively. Sweepback is found to be beneficial if either,

- (a) the static pressure in the trailing edge surface is greater than free-stream pressure, and the flow is directed outward,
- or,

(b) the static pressure is less than its free-stream value, and the flow is directed inward. If the static pressure is equal to that of the free-stream, sweepback has no effect.

It is shown how 'maps' of a given flow field may be drawn so as to indicate those parts which, from their lifting efficiency, seem most suitable for incorporation into an efficient lifting system.

Finally, a tentative proposal is made for utilising the new concepts in an experimental programme.

LIST OF SYMBOLS

f_L, f_D	Lift and drag functions defined by equations (8) to (11)
k	Function defined by equation (30)
l, m, n	Direction cosines of shock surface at point where streamline enters
p	Static pressure
q	$\frac{1}{2} \rho v^2$
r	Radius in cylindrical co-ordinates (x, r, ψ)
s	Entropy
v	Velocity
v_0	Velocity corresponding to $p = p_\infty$
v_{\max}	Velocity obtained by expansion into a vacuum
\bar{v}	v/v_{\max}
\bar{v}_0	v_0/v_{\max}
x, y, z	Rectangular co-ordinates, x streamwise, y spanwise, z vertical
A_b, A_c, A_e, A_p	Base, capture, entry and planform areas respectively
dA_e^*	Area intersected by elementary streamtube with plane normal to free-stream direction
C_L, C_D	Coefficients of lift and drag based on planform area
C_p	Pressure coefficient = $(p - p_\infty) / \frac{1}{2} \rho_\infty v_\infty^2$
D	Drag
E_s	Efficiency ratio, defined for streamlines by equation (27)
E_w	Efficiency ratio, defined for wings by equation (26)
L	Lift
M	Mach number
R	Gas constant
β	$(M^2 - 1)^{\frac{1}{2}}$
γ	Ratio of specific heats
δ	Streamline deflection angle
ϵ	Angle between streamline and x-axis, viewed in z-direction
θ	Angle between shock wave and x-axis
λ	Ratio of total pressures or densities
ρ	Density

LIST OF SYMBOLS—*continued*

ψ	Angle in cylindrical co-ordinates (x, r, ψ), $\psi = 0$ is vertically downward
Γ	Ratio of pressure to momentum terms in drag equation (Appendix B)
Λ	Angle between rear end of control volume and yz plane
<i>Suffices</i>	
b	Value in base plane
r	Radial component
t	Total values of pressure or density
w	Relating to a wing
W	Relating to a plane wedge
∞	Free-stream conditions
1	Conditions immediately behind shock wave
x, y, z	Components in x, y, z directions

Note: The variables $p, s, v, \bar{v}, \delta, \epsilon, \rho$, when used without any suffix, refer normally to conditions at the point where the streamline under consideration leaves the control volume. Exceptions to this rule should be clear from context.

REFERENCES

No.	Author(s)	Title, etc.
1	D. Küchemann	Hypersonic aircraft and their aerodynamic problems: <i>Progress in Aeronautical Sciences</i> , edited by D. Küchemann and L. H. G. Sterne, Vol. 6 pp. 271–353. Pergamon Press 1965.
2	T. R. F. Nonweiler	Delta wings of shapes amenable to exact shock wave theory. <i>J. Roy. Aero. Soc.</i> , Vol. 67 (1963).
3	J. G. Jones	A method for designing lifting configurations for high supersonic speeds using the flow fields of non-lifting cones. A.R.C. R. & M. 3539 (1963).
4	K. C. Moore	The application of known flow fields to the design of wings with lifting upper surfaces at high supersonic speeds. R.A.E. Technical Report 65034 (A.R.C. 26913) (1965).
5	J. Pike	A design method for aircraft basic shapes with fully attached shock waves using known axisymmetric flow fields. R.A.E. Technical Report 66069 (1966) A.R.C. 28292.
6	J. G. Jones K. C. Moore J. Pike P. L. Roe	A method for designing lifting configurations for high supersonic speeds using axisymmetric flow fields. <i>Ingenieur-Archiv</i> . Vol. XXXVII, Pt. 1, pp. 56–72, June 1968.

REFERENCES—*continued*

<i>No.</i>	<i>Author(s)</i>	<i>Title, etc.</i>
7	J. Pike	Minimum drag surfaces of given lift which support two-dimensional supersonic flow fields. A.R.C. R. & M. 3543 (1967).
8	R. S. Bartlett	High lift-drag ratio double wedges of given volume which support two-dimensional supersonic flow fields. R.A.E. Technical Report 66306 (A.R.C. 28826) (1966)
9	R. Courant	<i>Differential and integral calculus</i> , Vol. II. Blackie and Sons, London (1936).
10	K. C. Moore	Private communication.
11	B. A. Woods	The forces on a compression surface based on an axisymmetrical conical flow field. R.A.E. Technical Report 64035 (A.R.C. 26580) (1964).
12	P. J. Zandbergen	On the determination of optimum shapes with finite nose angles. NLR Amsterdam Report TR G.30 (1964).
13	R. S. Bartlett	Tables of supersonic symmetrical flow around right circular cones, with and without the addition of heat at the wave. A.R.C. R. & M. 3521 (1966).
14	R. F. Clippinger J. H. Giese W. C. Carter	Tables of supersonic flow about cone cylinders. Part II, Complete flows. Aberdeen Proving Ground Ballistic Research Laboratories Report 730 (P 30973) (1950).
15	S. Mölder	Lifting configurations for high supersonic speeds derived from internal axisymmetric conical flow fields. Mechanical Engineering Research Laboratories, McGill University, Montreal (1965).

APPENDIX A

Some Simple Oblique Shock Relationships.

Consider the flow past a two-dimensional wedge supporting an oblique shock as in Fig. 24. The following equations can be written immediately.

Conservation of x-momentum.

$$\rho_{\infty} v_{\infty}^2 \tan \theta = \rho v_x^2 (\tan \theta - \tan \delta) + (p - p_{\infty}) \tan \theta. \quad (\text{A.1})$$

Conservation of z-momentum.

$$(p - p_{\infty}) = \rho v_x^2 \tan \delta (\tan \theta - \tan \delta). \quad (\text{A.2})$$

Continuity.

$$\rho_{\infty} v_{\infty} \tan \theta = \rho v_x (\tan \theta - \tan \delta). \quad (\text{A.3})$$

These are not sufficient to solve the flow, because the energy equation and the equation of state have been omitted. However, they do permit some very simple relationships to be written which are useful at certain places in this Report. Using equation (A.3) to substitute for $(\tan \theta - \tan \delta)$ in equations (A.1) and (A.2) respectively, we obtain

$$(p - p_\infty) = \rho_\infty v_\infty (v_\infty - v_x) \quad (\text{A.4})$$

$$(p - p_\infty) = \rho_\infty v_\infty v_x \tan \theta \tan \delta. \quad (\text{A.5})$$

These equations evidently hold immediately behind a shock wave of any form or strength. The curious result (A.4) that the relationship between pressure coefficient and streamwise velocity perturbation is exactly the same as in linear theory appears to be little known. It is not generally true at large distances behind the shock.

APPENDIX B

The Orders of Magnitude of the Terms in the Drag Function

Consider the lift and drag functions for flow past a wing with an unswept trailing edge

$$f_L = \frac{2l}{n} \cdot \frac{v_z}{v_\infty} \quad (\text{B.1})$$

$$f_D = \frac{2l}{n} \left[\frac{v_\infty - v_x}{v_\infty} - \frac{p - p_\infty}{\rho v_\infty v_x} \right]. \quad (\text{B.2})$$

It is interesting to enquire whether there exist combinations of lift coefficient and Mach number such that one of the terms in (B.2) becomes negligible compared with the other; that is, does

$$\Gamma = \frac{p - p_\infty}{\rho v_x (v_\infty - v_x)} \quad (\text{B.3})$$

ever become either very large or very small? As a typical value we may calculate Γ immediately behind the shock, where use of equations (A.3) and (A.4) yields

$$\Gamma = \frac{\tan \theta - \tan \delta}{\tan \theta} \quad (\text{B.4})$$

which is always of order unity. It is, therefore, never legitimate to neglect either term in (B.2).

APPENDIX C

The Effect of Trailing Edge Sweep on a Double-Nonweiler Wing.

A very simple illustration of the qualitative relationship between spanwise velocity component, trailing edge sweep, and lifting efficiency, is provided by the following example. Consider the system formed by two plane shock waves intersecting along a line in the plane $y = 0$ (Fig. 25). Stream-surfaces drawn behind these shockwaves can be combined to form a 'double-Nonweiler' wing². Let the traces of the shock waves in planes $x = \text{const}$ make angle ψ with the horizontal. If θ is the inclination of the shock to the free-stream, and δ the flow deflection relative to the flow stream, we have

$$v_z = v_x \tan \delta \cos \psi$$

$$v_y = v_x \tan \delta \sin \psi$$

$$l/n = \tan \theta / \cos \psi .$$

If these relationships are substituted into equations (18) and (19), and further simplification carried out by use of the results in Appendix A, there is obtained, for any streamline,

$$\begin{aligned} f_L &= C_p \\ f_D &= \frac{C_p \tan \delta}{\cos \psi} \left[\frac{1 - \tan \Lambda \tan \theta \sin \psi}{1 - \tan \Lambda \tan \delta \sin \psi} \right] \end{aligned} \quad (C.1)$$

so that, for the entire wing,

$$\frac{L}{D} = \frac{f_L}{f_D} = \frac{\cos \psi}{\tan \delta} \left[\frac{1 - \tan \Lambda \tan \theta \sin \psi}{1 - \tan \Lambda \tan \delta \sin \psi} \right]. \quad (C.2)$$

Suppose Λ to be given. Then for small values of ψ , efficiency is enhanced by making $\Lambda\psi$ positive. It is easily shown by differentiating equation (C.2) that maximum (L/D) is achieved when $\tan \Lambda \sin \psi$ is the smallest positive root of the equation

$$ax^3 + bx^2 + cx + d = 0 \quad (C.3)$$

where

$$a = \tan \delta \tan \theta$$

$$b = -2 \tan \delta$$

$$c = 1$$

$$d = -\tan^2 \Lambda (\tan \theta - \tan \delta).$$

If ψ is given, the efficiency increases monotonically with Λ if ψ is positive, and decreases if ψ is negative. The limit is reached when the trailing edge becomes sonic, when the present method of analysis is no longer valid.

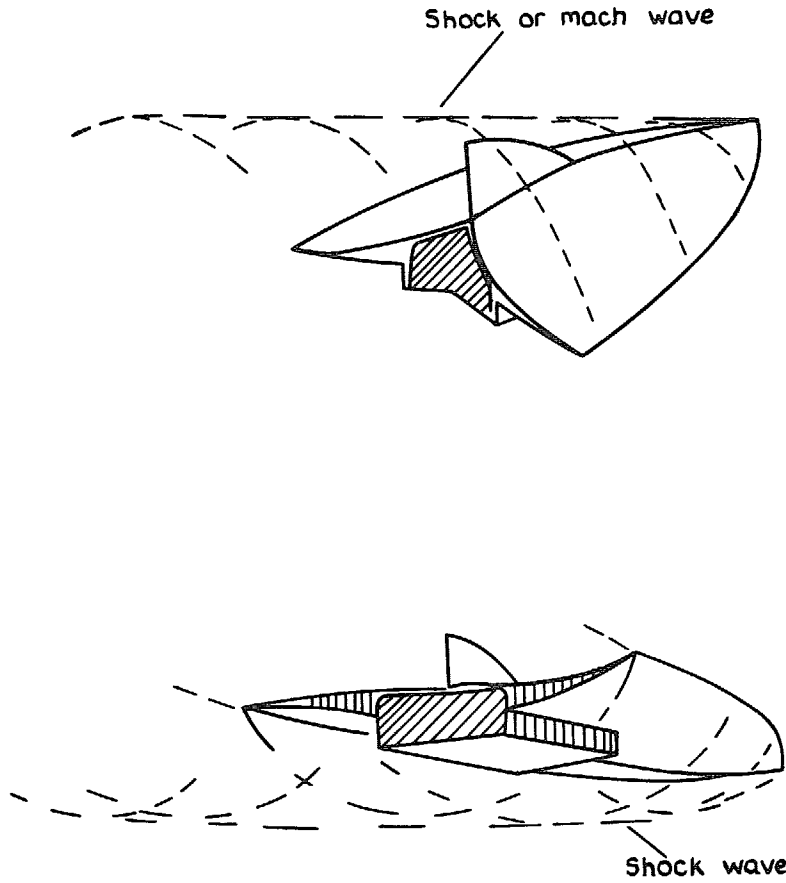


FIG. 1. A lifting shape with attached shock waves.

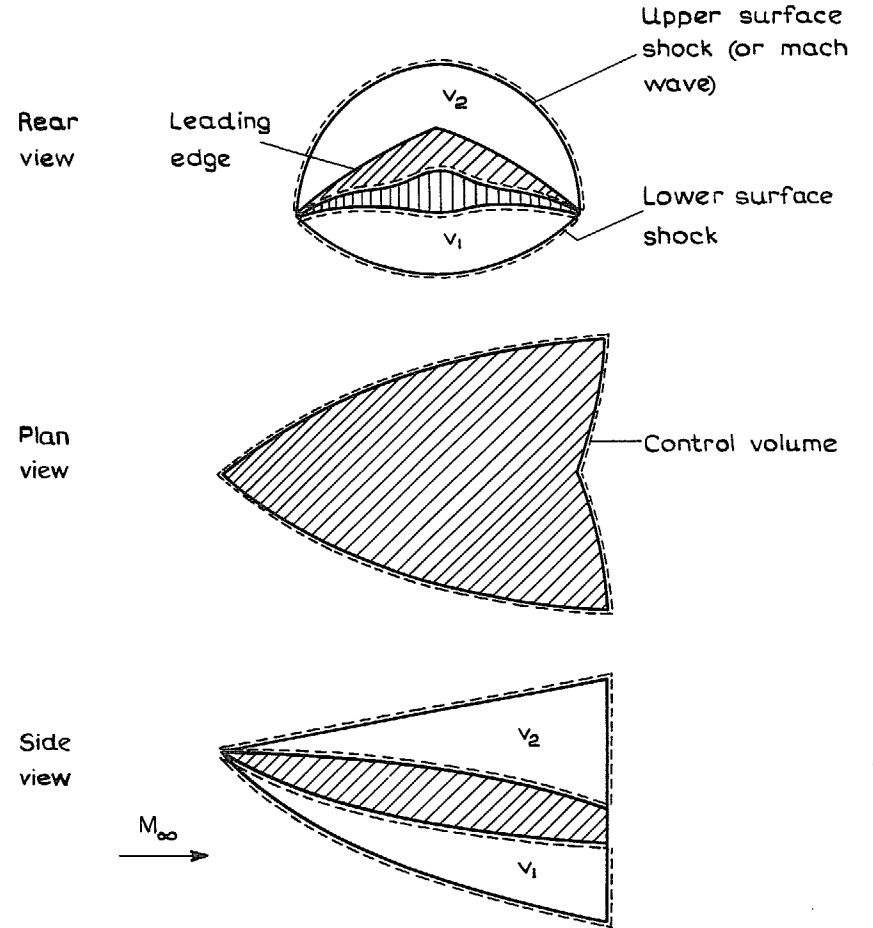


FIG. 2. A lifting shape and its associated control volumes.

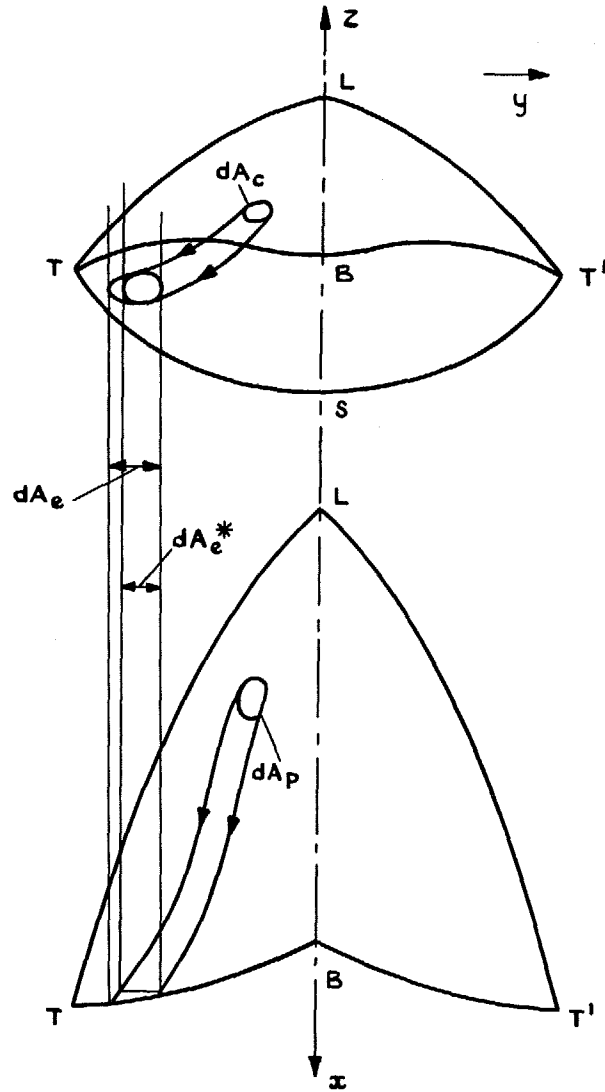
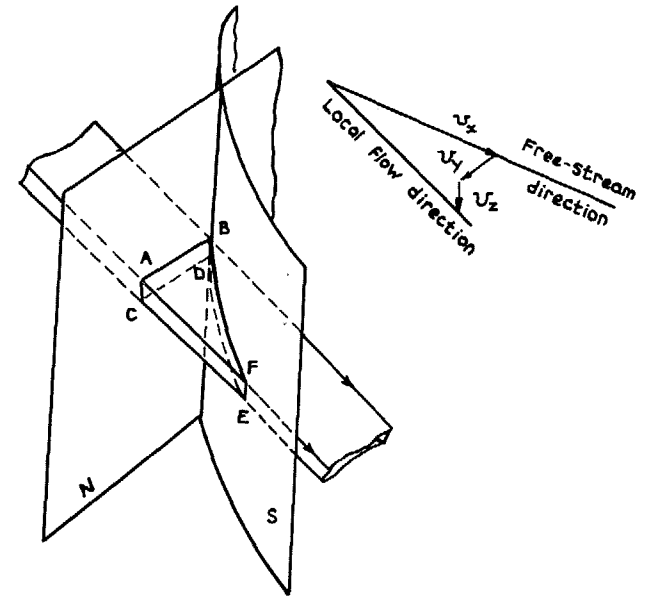
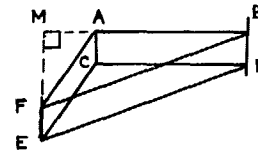


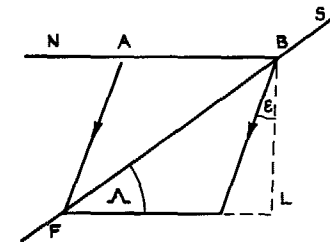
FIG. 3. The control volume for the lower surface.



(a) Perspective view



(b) View in direction of free-stream



(c) View in z-direction

FIG 4a to c. Streamtube passing through an oblique surface.

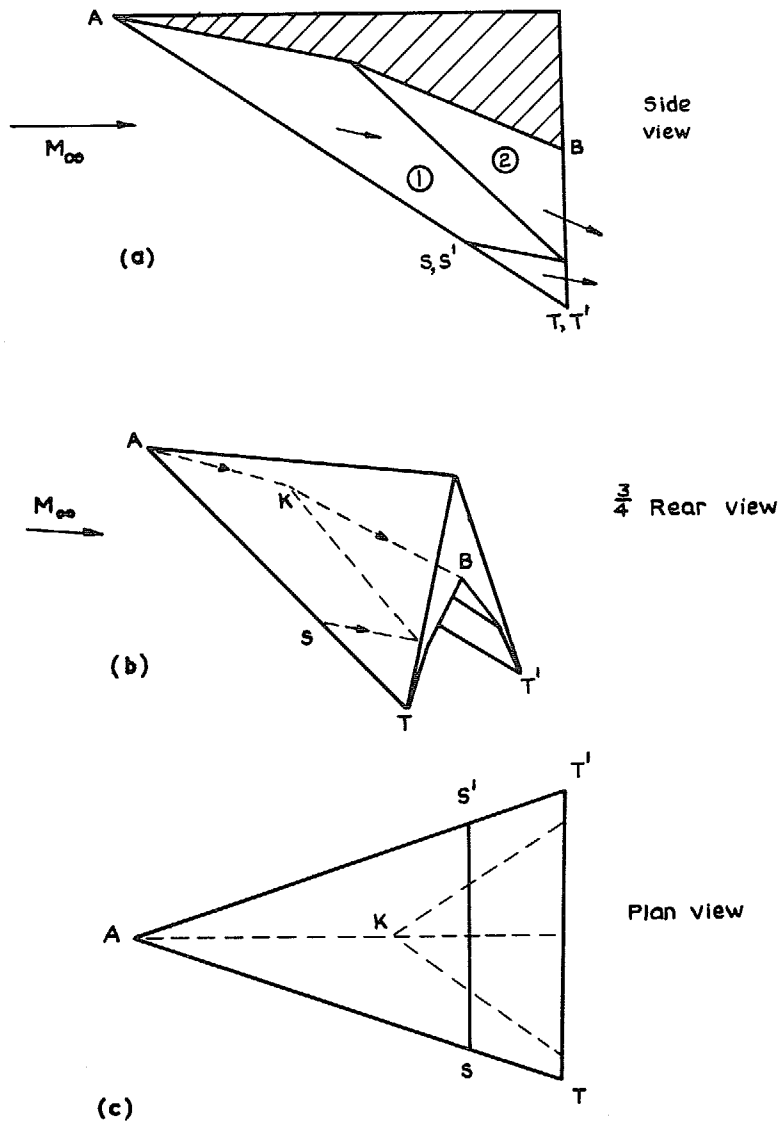


FIG 5a to c. A wing derived from the flow past a double-wedge.

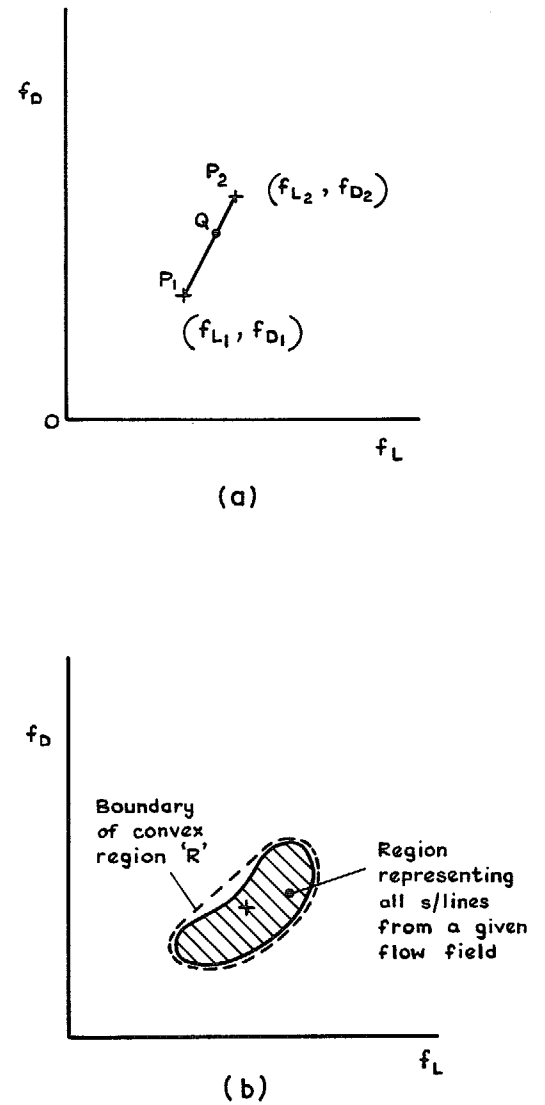


FIG. 6a & b. The lift-drag plane.

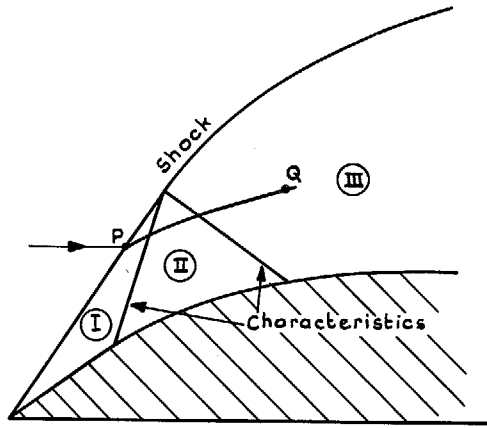


FIG. 7. General two-dimensional flow.

29

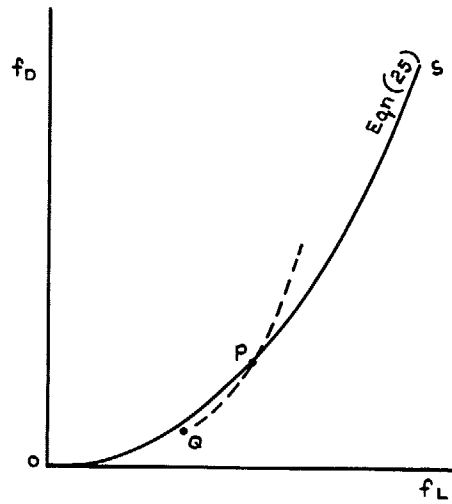


FIG. 8. Representation of Fig. 7 in lift-drag plane.

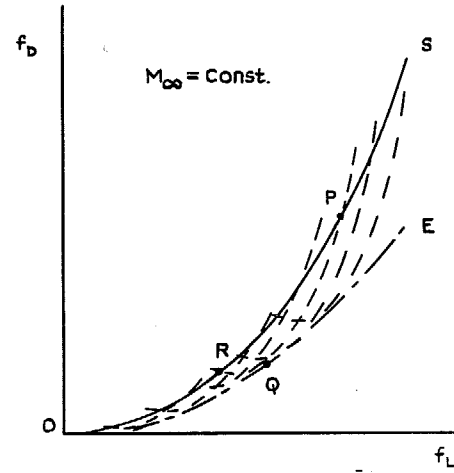


FIG. 9. Optimum relationships between f_L and f_D in two-dimensional flow.

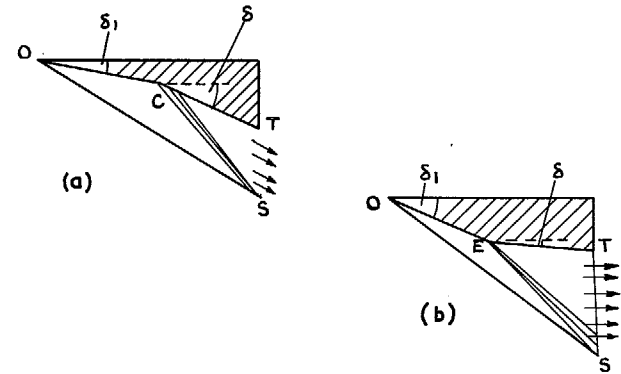


FIG. 10a & b. Optimum lifting shapes in two-dimensional flow.

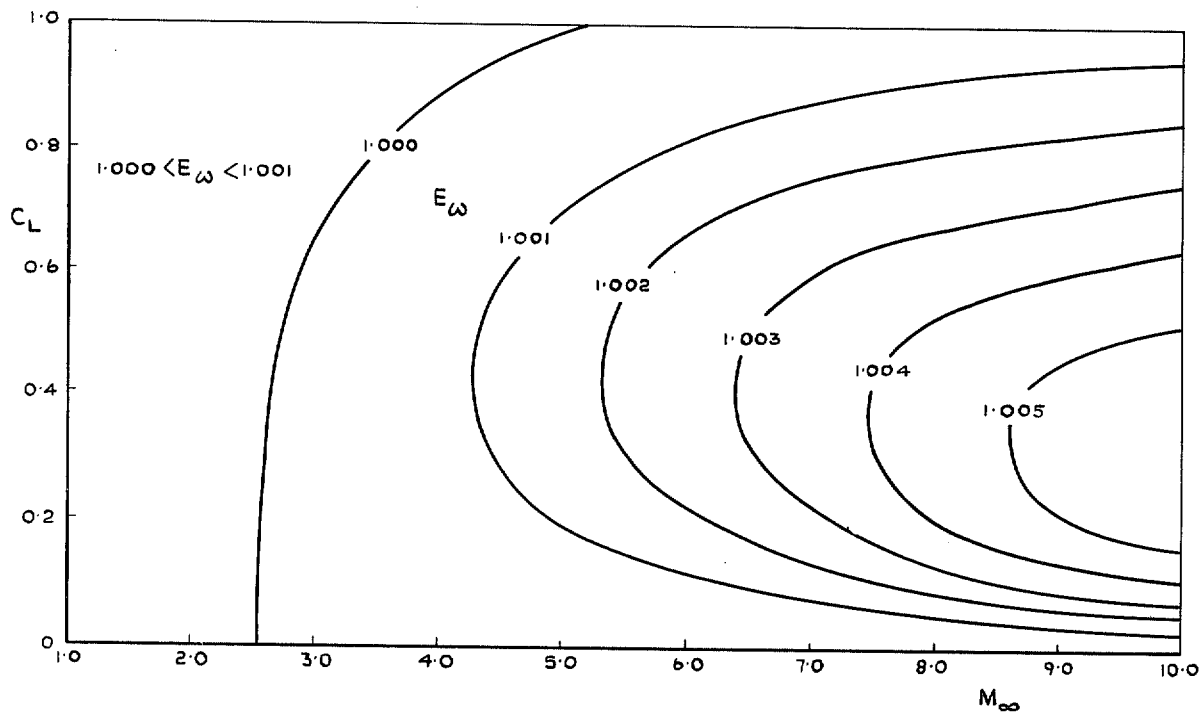


FIG. 11. Efficiency ratio for optimum two-dimensional wings.

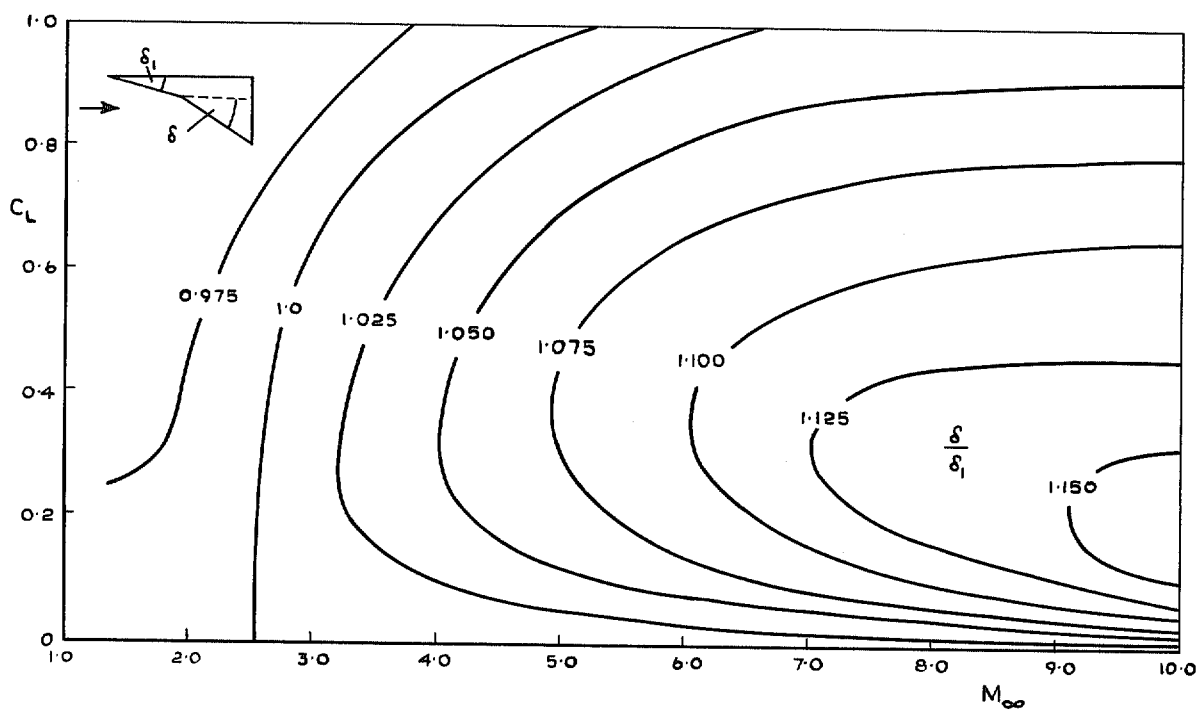


FIG. 12. Ratio of final to initial deflection angles for optimum two-dimensional lifting surfaces.

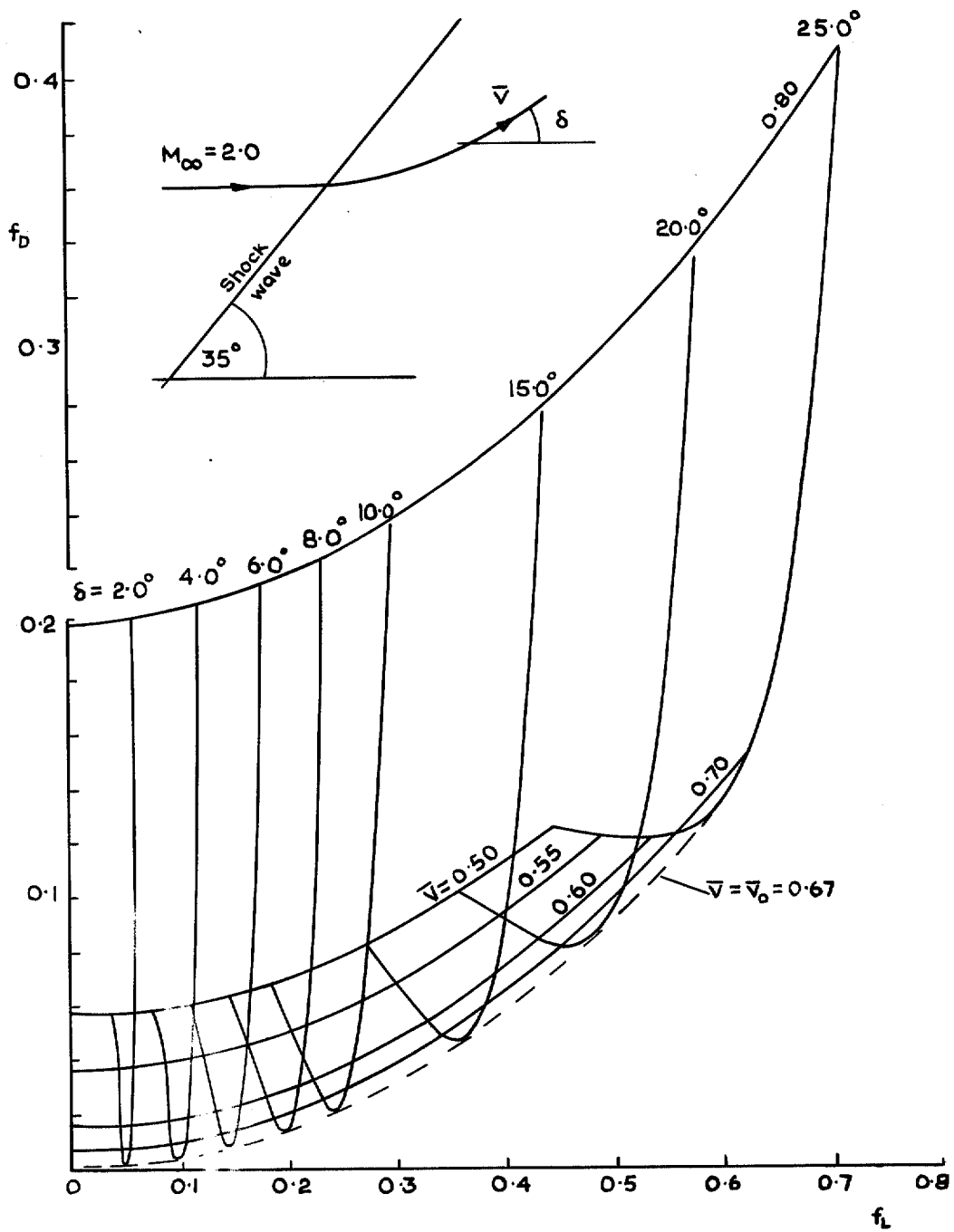


FIG. 13. Lifting properties of streamlines behind an oblique shock of given strength.

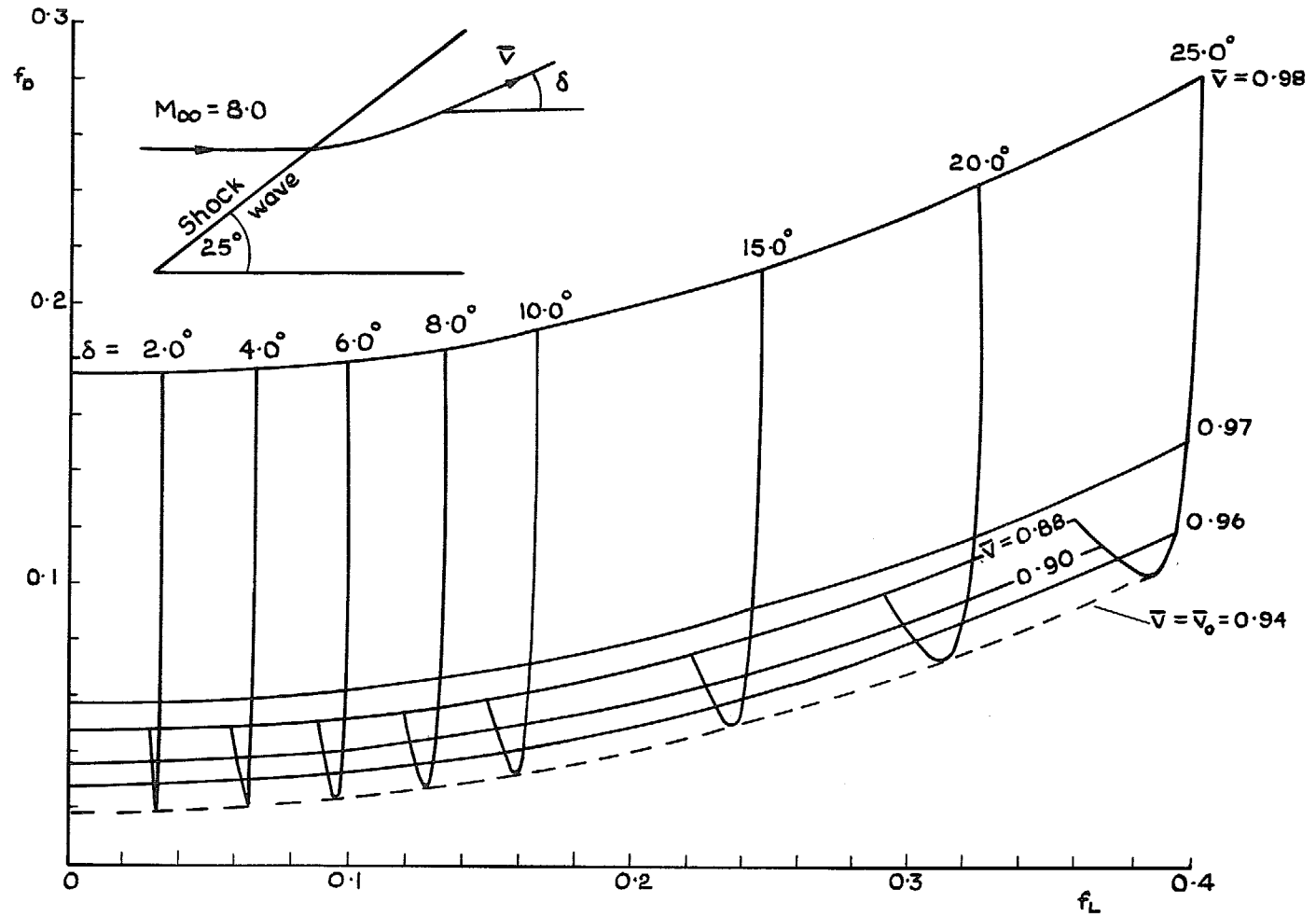


FIG. 13 contd. Lifting properties of streamlines behind an oblique shock of given strength.

$$M_\infty = \text{Const}$$

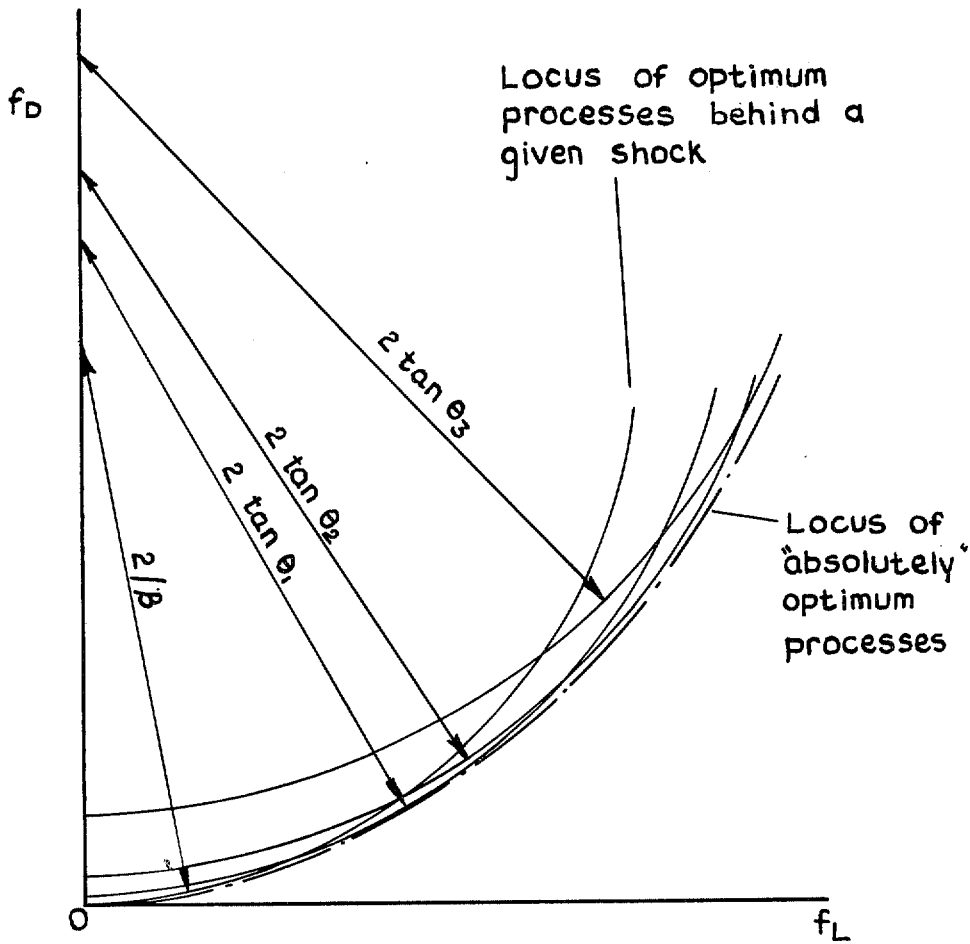


FIG. 14. Family of optimum loci.

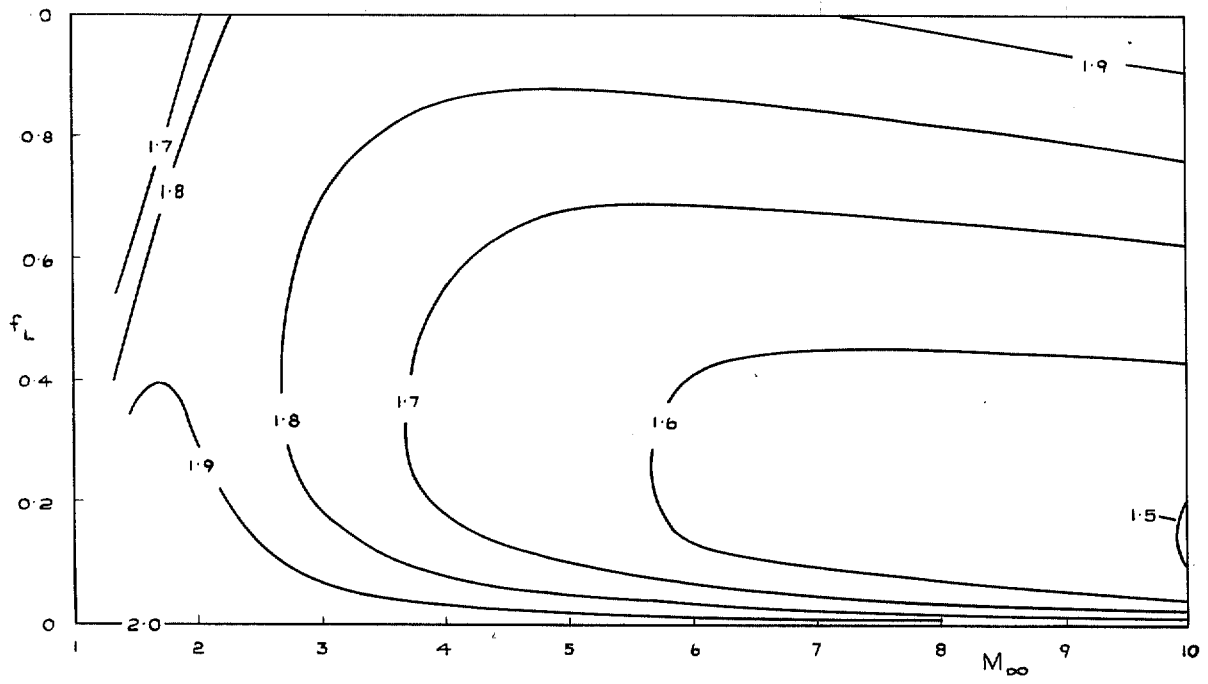


FIG. 15. Efficiency ratio E_s for optimum flow process.

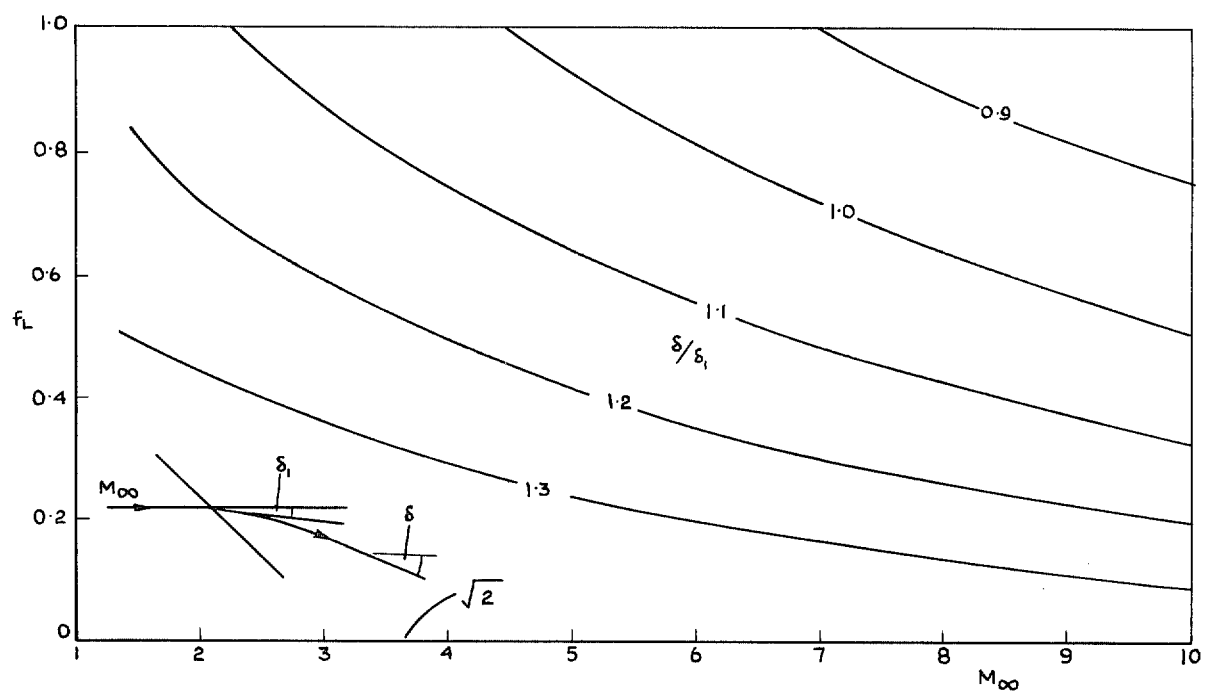


FIG. 16. Ratio of final to initial deflection for optimum flow process.

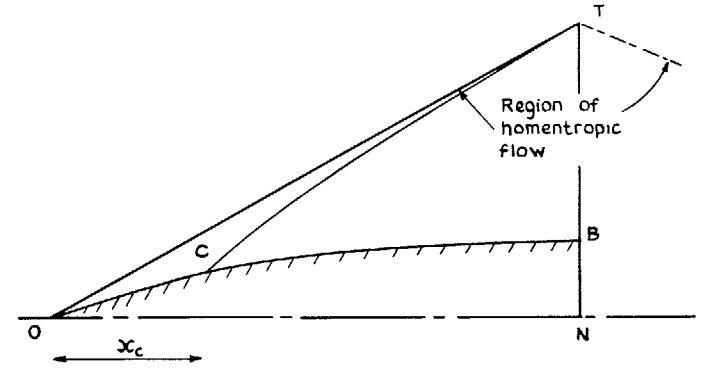
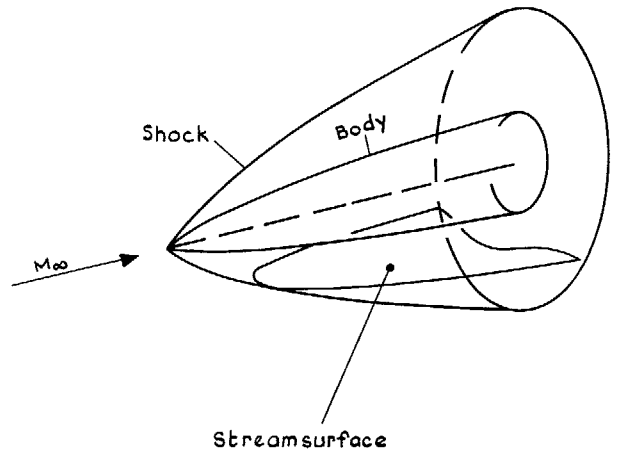


FIG. 18. Homentropic axisymmetric flow field.

35

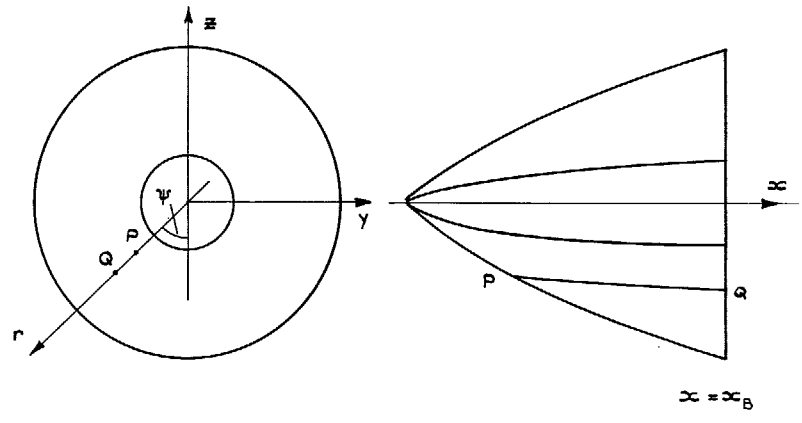


FIG. 17. The flow past an axisymmetric body.

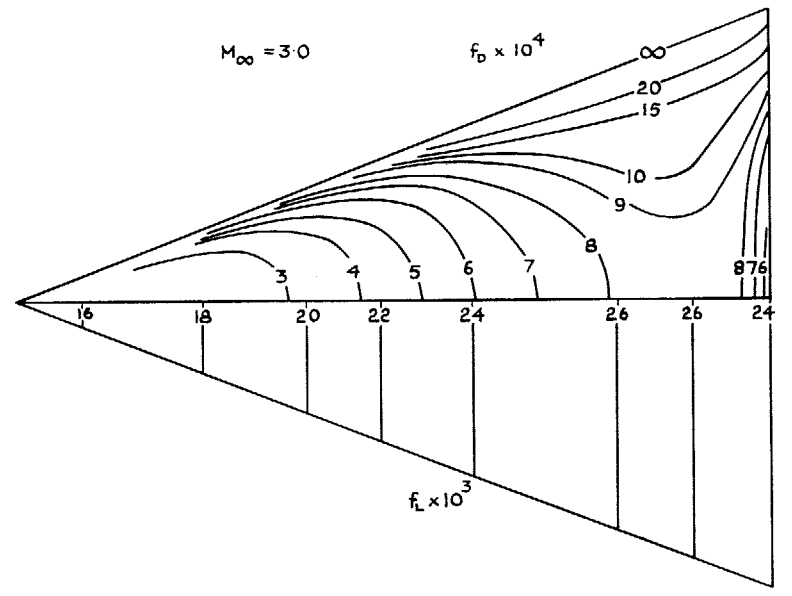


FIG. 19. Map of lift and drag functions for Moore's flow field.

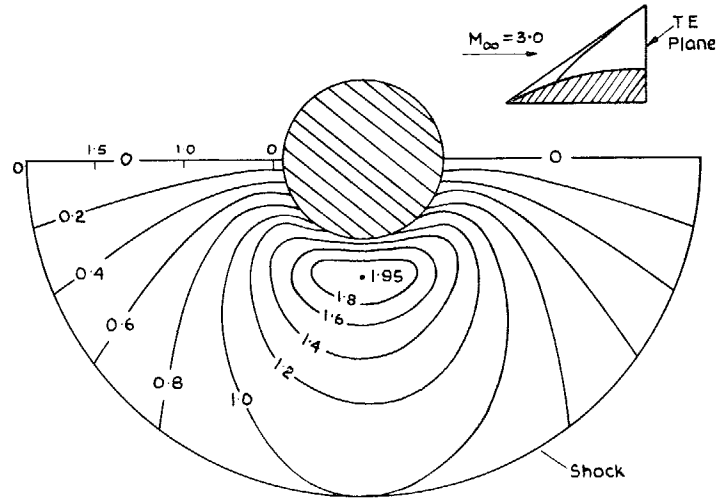


FIG. 20. Map of efficiency ratio for Moore's flow field.

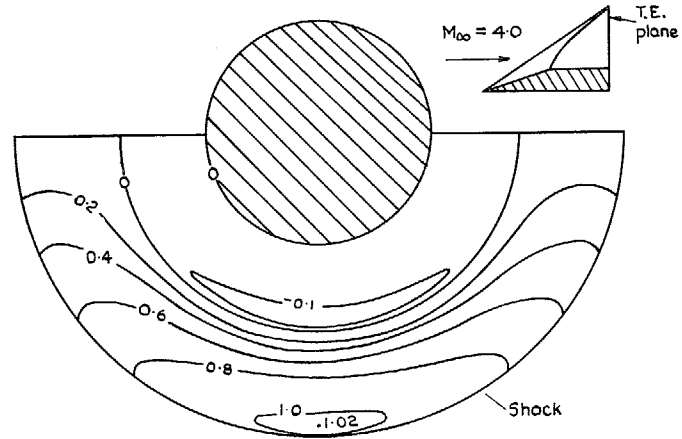
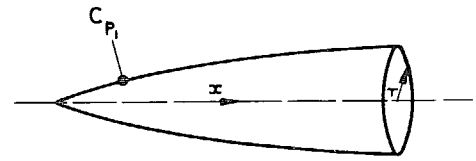
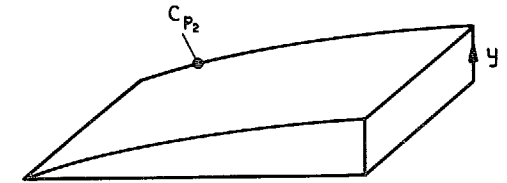


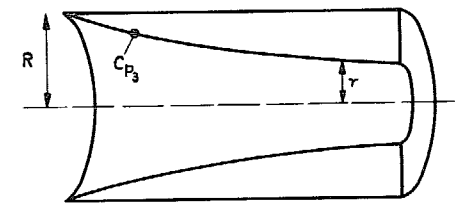
FIG. 21. Map of efficiency ratio for 10° cone-cylinder.



Axisymmetric body $r = f(x)$



Two-dimensional body $y = f(x)$



Axisymmetric duct $(R - r) = f(x)$
 At corresponding x -stations
 $C_{P_1} < C_{P_2} < C_{P_3}$

FIG. 22. Illustrating different types of flow field.

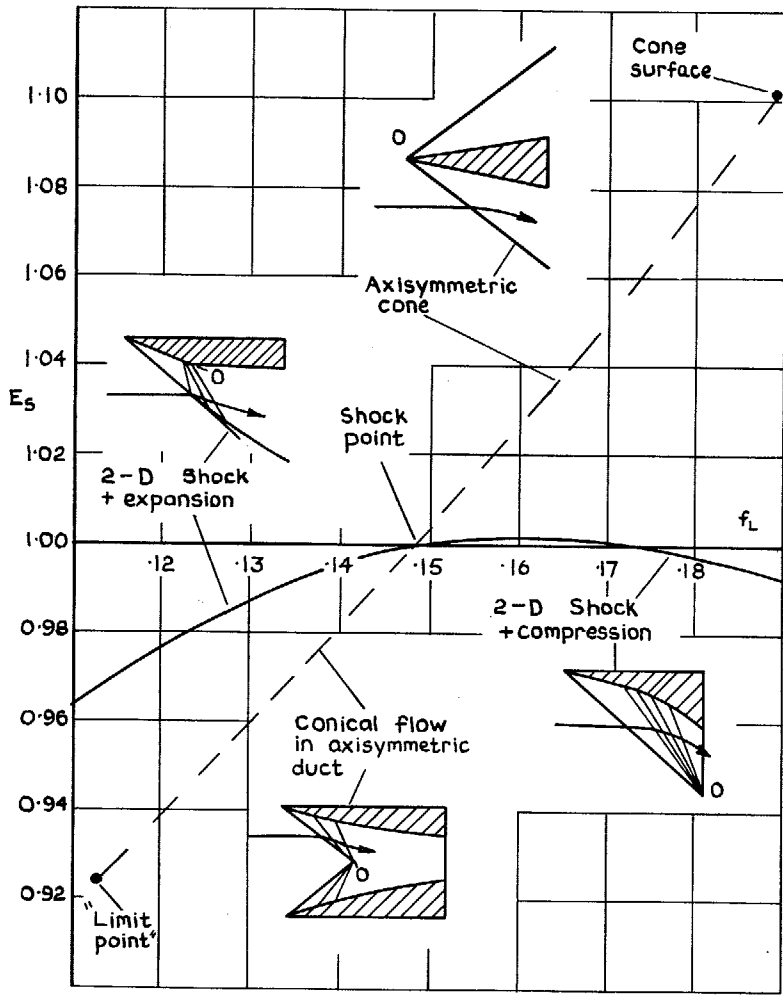


FIG. 23. A comparison of four conical flowfields.

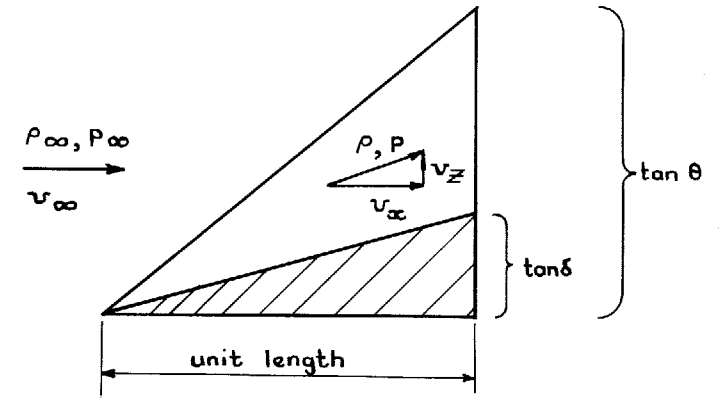


FIG. 24. Supersonic flow past a wedge.

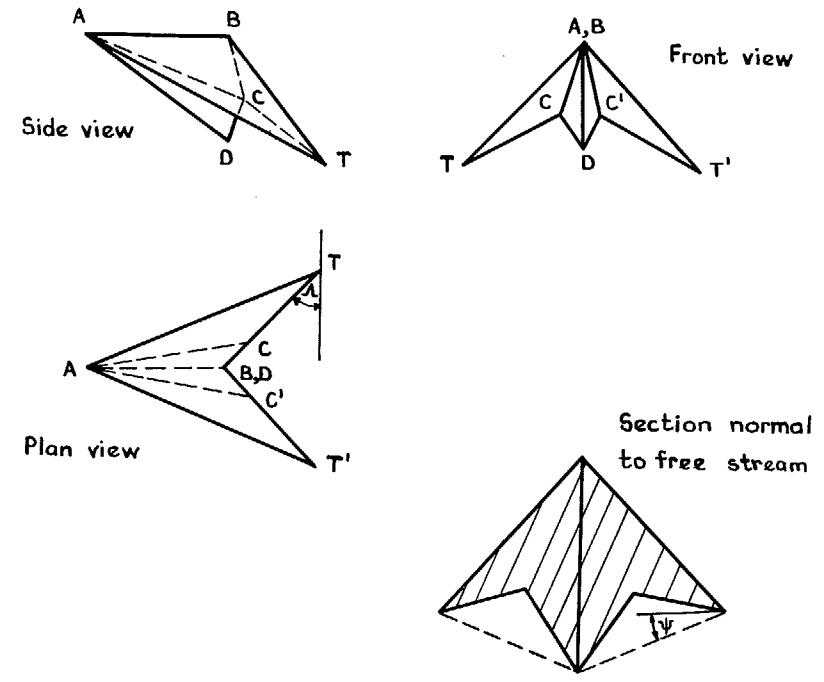


FIG. 25. Double Nonweiler wing with swept trailing edge.

Printed in Wales for Her Majesty's Stationery Office by Allens Printers (Wales) Ltd.

Dd. 135646 K.5

© Crown copyright 1969

Published by
HER MAJESTY'S STATIONERY OFFICE

To be purchased from
49 High Holborn, London W.C.1
13A Castle Street, Edinburgh 2
109 St. Mary Street, Cardiff CF1 1JW
Brazennose Street, Manchester M60 8AS
50 Fairfax Street, Bristol BS1 3DE
258 Broad Street, Birmingham 1
7 Linenhall Street, Belfast BT2 8AY
or through any bookseller